3. Curran ME, Splawski I, Timothy KW, Vincent GM, Green ED, Keating MT. A molecular basis for cardiac arrhythmia: HERG mutations cause long QT syndrome. Cell 1995;80:795–803.
4. Sanguinetti MC, Jiang C, Curran ME, Keating MT. A mechanistic link between an inherited and an acquired cardiac arrhythmia: HERG encodes the IKr potassium channel. Cell 1995;81:299–307.
5. January CT, Gong Q, Zhou Z. Long QT syndrome: cellular basis and arrhythmia mechanism in LQT2. J Cardiovasc Electrophysiol 2000; 11:1413–8.
6. Ficker E, Dennis AT, Obejero-Paz CA, Castaldo P, Taglialatela M, Brown AM. Retention in the endoplasmic reticulum as a mechanism of dominant-negative current suppression in human long QT syndrome. J Mol Cell Cardiol 2000;32:2327–37.
7. Sanguinetti MC, Tristani-Firouzi M. hERG potassium channels and cardiac arrhythmia. Nature 2006;440:463–9.
8. Anderson CL, Delisle BP, Anson BD, et al. Most LQT2 mutations reduce Kv11.1 (hERG) current by a class 2 (trafficking-deficient) mechanism. Circulation 2006;113:365–73.
9. Moss AJ, Zareba W, Kaufman ES, et al. Increased risk of arrhythmic events in long-QT syndrome with mutations in the pore region of the human ether-a-go-go-related gene potassium channel. Circulation 2002;105:794–9.
10. McConkey EH. Mutation qualitative aspects. In: McConkey EH, editor. Human Genetics: The Molecular Revolution. Boston, MA: Jones and Bartlett, 1993:139–59.
11. Moss AJ, Shimizu W, Wilde AA, et al. Clinical aspects of type-1 long-QT syndrome by location, coding type, and biophysical function of mutations involving the KCNQ1 gene. Circulation 2007;115: 2481–9.
12. Nagaoka I, Shimizu W, Itoh H, et al. Mutation site dependent variability of cardiac events in Japanese LQT2 form of congenital long-QT syndrome. Circ J 2008;72:694–9.
13. Splawski I, Shen J, Timothy KW, et al. Spectrum of mutations in long-QT syndrome genes. KVLQT1, HERG, SCN5A, KCNE1, and KCNE2. Circulation 2000;102:1178–85.
14. Swiss Institute of Bioinformatics. UniProtKB/Swiss-Prot: KCNH2_HUMAN (Q12809). Available at: http://ca.expasy.org/cgi-bin/ft_viewer.pl?Q12809. Accessed October 19, 2009.
15. Cox DR. Regression models and life-tables. J Stat Soc [B] 1972;34: 187–220.
16. Lin DY, Wei LJ. The robust inference for the proportional hazards model. J Am Stat Assoc 1989;84:1074–8.
17. Wang Q, Shen J, Splawski I, et al. SCN5A mutations associated with an inherited cardiac arrhythmia, long QT syndrome. Cell 1995;80: 805–11.
18. Roden DM. Clinical practice. Long-QT syndrome. N Engl J Med 2008;358:169–76.
19. Ueda K, Valdivia C, Medeiros-Domingo A, et al. Syntrophin mutation associated with long QT syndrome through activation of the nNOS-SCN5A macromolecular complex. Proc Natl Acad Sci U S A. 2008;105:9355–60.
20. Wu G, Ai T, Kim JJ, et al. Alpha-1-syntrophin mutation and the long QT syndrome: a disease of sodium channel disruption. Circ Arrhythmia Electrophysiol 2008;1:193–201.
21. Zareba W, Moss AJ, Schwartz PJ, et al. Influence of the genotype on the clinical course of the long-QT syndrome. N Engl J Med 1998; 339:960–5.
22. Wilde AA, Jongbloed RJ, Doevendans PA, et al. Auditory stimuli as a trigger for arrhythmic events differentiate HERG-related (LQT2) patients from KVLQT1-related patients (LQT1). J Am Coll Cardiol 1999;33:327–32.
23. Schwartz PJ, Priori SG, Spazzolini C, et al. Genotype-phenotype correlation in the long-QT syndrome: gene-specific triggers for life-threatening arrhythmias. Circulation 2001;103:89–95.
24. Priori SG, Schwartz PJ, Napolitano C, et al. Risk stratification in the long-QT syndrome. N Engl J Med 2003;348:1866–74.
25. Shimizu W, Noda T, Takaki H, et al. Diagnostic value of epinephrine test for genotyping LQT1, LQT2 and LQT3 forms of congenital long QT syndrome. Heart Rhythm 2004;1:276–83.
26. Zareba W, Moss AJ, Sheu G, et al. Location of mutation in the KCNQ1 and phenotypic presentation of long QT syndrome. J Cardiovasc Electrophysiol 2003;14:1149–53.
27. Shimizu W, Horie M, Ohno S, et al. Mutation site-specific differences in arrhythmic risk and sensitivity to sympathetic stimulation in LQT1 form of congenital long QT syndrome. Multi-center study in Japan. J Am Coll Cardiol 2004;44:117–25.
28. Gong Q, Zhang L, Vincent GM, Horne BD, Zhou Z. Nonsense mutations in hERG cause a decrease in mutant mRNA transcripts by nonsense-mediated mRNA decay in human long-QT syndrome. Circulation 2007;116:17–24.
29. Moss AJ, Zareba W, Hall WJ, et al. Effectiveness and limitations of beta-blocker therapy in congenital long-QT syndrome. Circulation 2000;101:616–23.
30. Priori SG, Napolitano C, Schwartz PJ, et al. Association of long QT syndrome loci and cardiac events among patients treated with beta-blockers. JAMA 2004;292:1341–4.
31. Shimizu W, Antzelevitch C. Differential effects of beta-adrenergic agonists and antagonists in LQT1, LQT2 and LQT3 models of the long QT syndrome. J Am Coll Cardiol 2000;35:778–86.

Key Words: arrhythmia ■ electrocardiography ■ long QT syndrome ■ genetics ■ syncope.

APPENDIX

For a table on the *KCNH2* mutations by location, coding type, and topology of mutation, and contributing registry, please see the online version of this article.

CONTEMPORARY REVIEW

Arrhythmias originating from the right ventricular outflow tract: How to distinguish "malignant" from "benign"?

Wataru Shimizu, MD, PhD

From the Division of Cardiology, Department of Internal Medicine, National Cardiovascular Center, Suita, Japan.

Idiopathic ventricular tachycardia (VT) originating from the right ventricular outflow tract (RVOT) in patients without structural heart diseases is generally considered as a benign ventricular arrhythmia (VA). However, "malignant" VA, ventricular fibrillation (VF), and/or polymorphic VT are occasionally initiated by VT or ventricular premature contraction (VPC) originating from the RVOT. In this review article, previous reports describing the malignant form of idiopathic RVOT VT are reviewed, and it is discussed how to distinguish the malignant form from the "benign" form of idiopathic VT originating from the RVOT.

KEYWORDS Ventricular fibrillation; Polymorphic ventricular tachycardia; Sudden death; Catheter ablation

(Heart Rhythm 2009;6:1507–1511)

Introduction

Ventricular tachycardia (VT) and ventricular premature contraction (VPC) originating from the right ventricular outflow tract (RVOT) are often observed in patients without structural heart diseases and are generally considered as benign ventricular arrhythmias (VAs).[1,2] It is important to distinguish an idiopathic RVOT VT from a VT caused by structural heart diseases, such as arrhythmogenic right ventricular dysplasia (ARVD), in which the RVOT is one of the origins of malignant VT.[3] The diagnosis of ARVD can be accomplished by demonstrating morphological abnormalities of the right ventricle with cardiac imaging, that is, echocardiography, magnetic resonance imaging (MRI)[4] or computed tomography, and so on. However, it is not always easy to detect subtle right ventricular (RV) morphological abnormalities at an early stage with cardiac imaging.[4] Idiopathic VT originating from the RVOT shows a left bundle-branch block configuration in the precordial leads and an inferior axis (normal axis or right axial deviation) in the limb leads (Figure 1A). Radiofrequency catheter ablation has become a primary therapy for idiopathic VT originating from the RVOT[2]; the success rates are approximately 90%, and the recurrence rates are generally low.[5–7] Approximate localization of the VT origin can be estimated by the QRS configuration during VT or VPC. Septal origin in the RVOT is suggested by QRS duration <140 ms, whereas free-wall origin is suggested by QRS duration ≥ 140 ms associated with notches in the downslope of QRS in inferior leads (II, III, aVF).[8,9] Deeper S waves in aVR lead than in aVL lead indicate rightward inferior origin, while deeper S waves in aVL than in aVR indicate leftward superior origin. Precise localization of the VT origin in the RVOT for radiofrequency catheter ablation is determined by the combined use of pace mapping during sinus rhythm and activation mapping during VT or VPC in electrophysiological study.

Idiopathic VT originating from the RVOT usually shows a monomorphic pattern of VT (Figure 1A), with nonsustained VT separated by several sinus beats and frequent VPCs. Idiopathic VT is generally catecholamine sensitive and is often induced with exercise or infusion of catecholamine, such as isoproterenol and epinephrine. The mechanism of idiopathic RVOT VT is thought to be triggered activity due to cAMP-mediated delayed afterdepolarizations; therefore, adenosine or adenosine triphosphate is effective in terminating RVOT VT.[5,10] β-Blockers are generally believed to be effective in preventing the recurrence of RVOT VT.

Although idiopathic VT originating from RVOT is generally considered benign (Figure 1A), more malignant ventricular arrhythmias, ventricular fibrillation (VF), and/or polymorphic VT are occasionally initiated by VT or VPC originating from RVOT[11–14] (Figure 1B, 1C). In this contemporary review, previous reports demonstrating the malignant form of idiopathic VT originating from the RVOT are reviewed, and it is discussed how to distinguish the malignant form from the benign form of idiopathic VT originating from RVOT.

Dr. Shimizu was supported in part by a health sciences research grant (H18, Research on Human Genome, 002) and the Research Grant for the Cardiovascular Diseases (21C-8) from the Ministry of Health, Labour and Welfare, Japan. **Address reprint requests and correspondence:** Dr. Wataru Shimizu, Division of Cardiology, Department of Internal Medicine, National Cardiovascular Center, 5-7-1 Fujishiro-dai, Suita, Osaka, 565-8565 Japan. E-mail address: wshimizu@hsp.ncvc.go.jp. (Received March 31, 2009; accepted June 8, 2009.)

1547-5271/$ -see front matter doi:10.1016/j.hrthm.2009.06.017

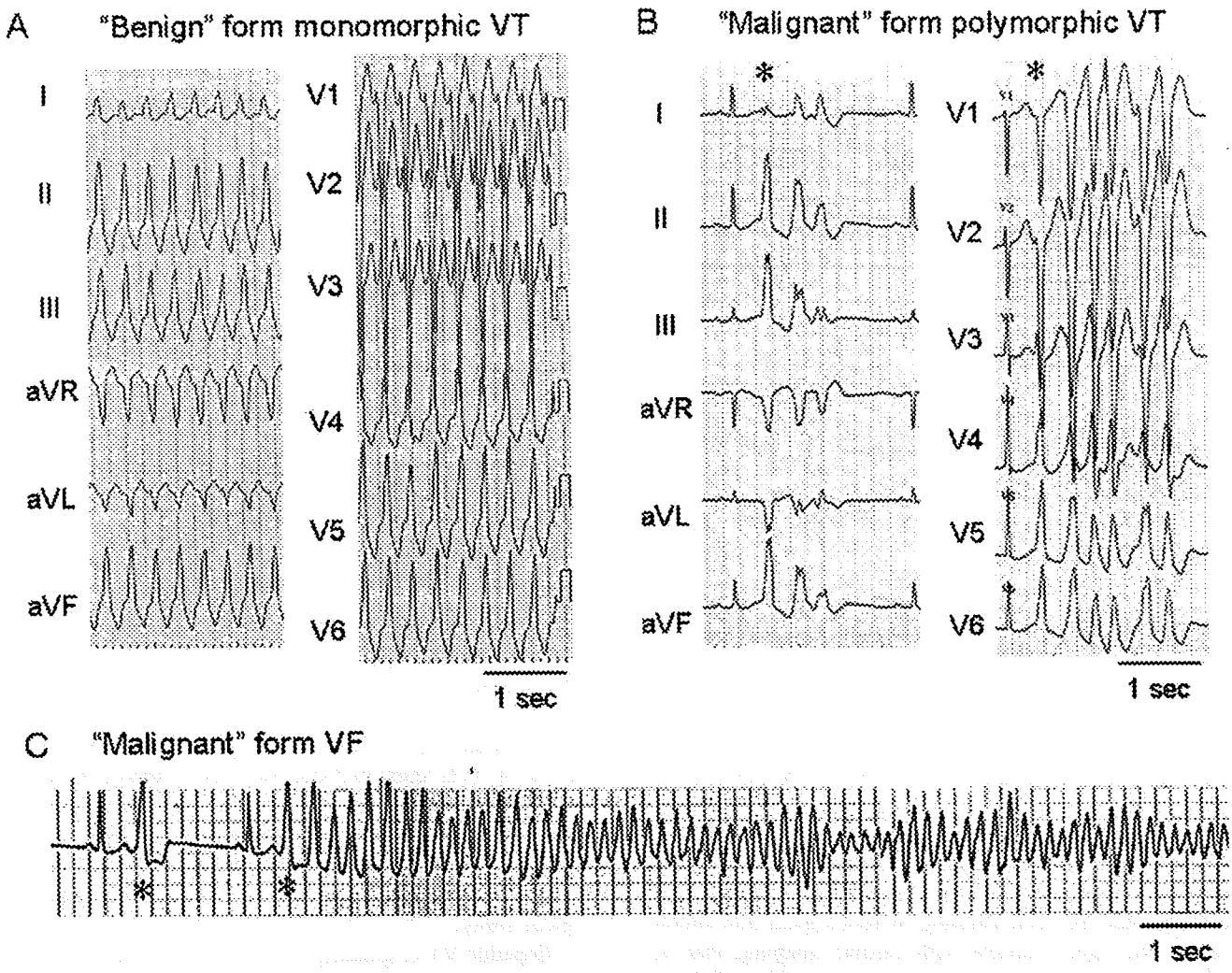

Figure 1 **A:** Twelve-lead ECG of benign form of idiopathic monomorphic VT originating from RVOT showing left bundle branch morphology with normal axis. **B:** Twelve-lead ECG of malignant form of idiopathic polymorphic VT originating from RVOT. Note that the initiating VPC showed left bundle branch morphology with inferior axis (*asterisks*). **C:** Initiation of VF recorded by a monitoring ECG in a patient with the malignant form of idiopathic VT originating from RVOT. Note that the QRS morphology of the initiating VPC was identical to that of the preceding isolated VPC (*asterisks*). Modified from reference 13 with permission.

Malignant form of idiopathic VT originating from RVOT: Previous reports

Since the late 1980s, idiopathic VF or polymorphic VT has been systematically reported in patients without organic heart disease or any identifiable etiology.[15,16] It is reported that such malignant VF or polymorphic VT is commonly initiated by a VPC with a very short coupling interval (CI). The morphologies of the initiating VPCs have been reported several times, and most showed a left bundle branch block (LBBB) pattern with a superior axis,[16] suggesting that the origin of the VPCs, which initiate VF or polymorphic VT, were the RV apex or RV inferior wall. In 1994, Leenhardt and coworkers[16] reported 14 patients with a new electrocardiographic (ECG) entity of a short-coupled variant of torsades de pointes, among whom the configuration of most of the initiating VPC was an LBBB pattern with a superior axis. In only one patient, the configuration of the initiating VPC was a LBBB pattern with a right axial deviation; however, the origin of the initiating VPC was not clearly suggested to be in the RVOT. To the best of our knowledge, Haissaguerre et al[11] were the first to demonstrate that the origin of VPCs initiating idiopathic VF was the RVOT in a minority of patients from their series. They recruited 27 patients who were resuscitated from recurrent episodes of primary idiopathic VF. The first initiating VPCs were observed during the electrophysiologic study and could be mapped in all 27 patients. The origin of the VPCs was mapped in the RVOT in four of 27 patients, and the VPCs were successfully eliminated by radiofrequency catheter ablation. Viskin and coworkers[12] described three patients who originally presented with typical benign-looking VT originating from RVOT but who developed malignant polymorphic VT during follow-up. Noda and coworkers[13] enrolled 16 patients who showed spontaneous VF (n = 5) or polymorphic VT (n = 11) initiated by VPC originating from RVOT among 101 consecutive patients

Table 1 Comparison of ECG characteristics between malignant RVOT VT, benign RVOT VT, and idiopathic VF

	Malignant RVOT VT	Benign RVOT VT	Idiopathic VF	*P*
CI, ms:				
Haissaguerre et al.	355 ± 30	—	280 ± 26	.01
Viskin et al.	340 ± 30	427 ± 76	300 ± 40	<.001
Noda et al.	409 ± 62	428 ± 65	—	.27
QRS duration, ms:				
Haissaguerre et al.	145 ± 12	—	126 ± 18	.04
Noda et al.	148 ± 8	142 ± 12	—	.03
Cycle length of VT, ms:				
Noda et al.	245 ± 28	328 ± 65	—	<.0001

in whom radiofrequency catheter ablation was conducted for treatment of VT or VPCs arising from RVOT. Our data indicated that the malignant form of idiopathic VT was present in 16% of the patients with idiopathic VT originating from RVOT; however, this high percentage represents a referral bias, since patients with the malignant form of idiopathic VT are more likely to be hospitalized and more likely to be referred for radiofrequency catheter ablation, while patients with the benign form of idiopathic VT are more likely to be treated conservatively as outpatients; therefore, the true frequency of the malignant form of idiopathic VT originating from RVOT is unknown but is much lower than 16%. Several patients with idiopathic VF have been reported as case reports, in which the initiating VPCs originated from RVOT could be successfully abolished by radiofrequency catheter ablation.[17–19]

How can we distinguish the malignant form from the benign form of idiopathic VT originating from RVOT?

Malignant ventricular arrhythmias, VF, and/or polymorphic VTs are sometimes associated with idiopathic VT or VPCs, which originate from RVOT. It is of particular importance to distinguish the malignant form from the benign form of idiopathic VT originating from RVOT, since the malignant form of idiopathic VT or VPCs often leads to unexpected sudden cardiac death.[11–13]

Several differences in ECG characteristics have been reported between malignant and benign forms of idiopathic VT. Some reports have suggested a relatively short CI of initiating VPCs, which arise from RVOT and result in malignant VF or polymorphic VT. Haissaguerre et al[11] divided 27 patients with idiopathic VF into two groups according to the origin of the initiating VPCs: VPCs elicited from the Purkinje conduction system in 23 patients and those originating from the myocardium at RVOT in four patients. They compared several ECG parameters of initiating VPCs between groups, although these parameters were not compared with the benign form of idiopathic VT arising from RVOT. The CIs of the initiating VPCs were short in both groups but were longer in idiopathic VF originating from RVOT than from the Purkinje system (355 ± 30 vs. 280 ± 26 ms; $P = .01$[11]; Table 1). In the three patients with malignant RVOT VT reported by Viskin and coworkers,[12] the CI of VPCs in three patients (340 ± 30 ms) was longer than that of VPCs in idiopathic VF (300 ± 40 ms) but shorter than that of VPCs in benign RVOT VT (427 ± 76 ms; Table 1). Moreover, when both monomorphic and polymorphic VT were recorded in the same patient, the CI leading to polymorphic VT was shorter than that leading to monomorphic VT. In the report by Noda and coworkers,[13] the CI of initiating VPCs in malignant RVOT VT was also short compared with the CI in benign RVOT VT (409 ± 62 vs. 428 ± 65 ms), although this did not reach statistical significance (Table 1). Thus, the available data suggest that the shorter CI of initiating VPCs correlates with the more malignant form of RVOT VT but that a cutoff value that would reliably differentiate malignant RVOT VT from benign RVOT VT remains to be defined. Moreover, long CI does not necessarily guarantee absence of risk.

The average QRS duration of the initiating VPCs originating from the RVOT in the malignant form of RVOT VT was reported to be 145 ± 12 ms by Haissaguerre et al[11] and

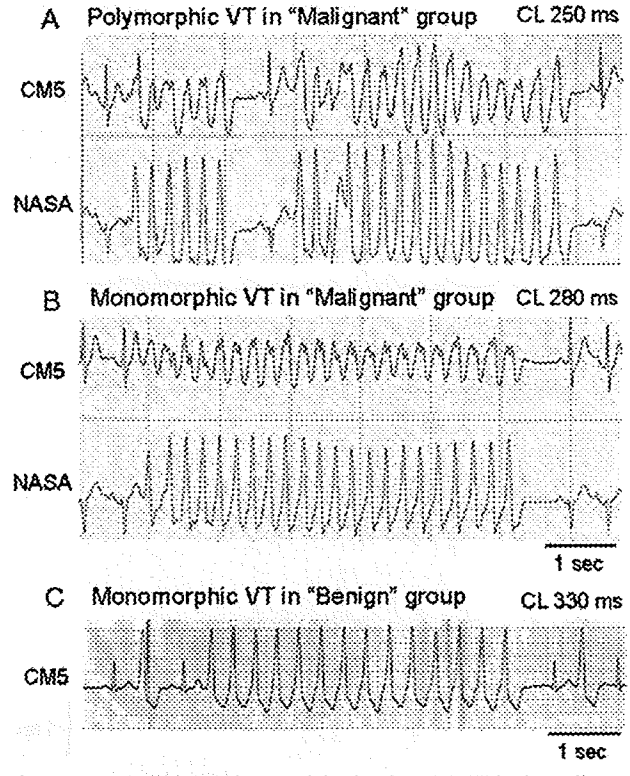

Figure 2 **A:** Polymorphic VT originating from RVOT in the malignant group on monitoring ECG. **B:** Monomorphic VT observed in the same malignant group patient as shown in panel **A**. **C:** Monomorphic VT originating from RVOT in the benign group. Note that the CL of monomorphic VT in the malignant group patient (280 ms) in panel **B** was longer than that of polymorphic VT in the same malignant group patient (250 ms) in panel **A**; however, it was shorter than that of monomorphic VT in the benign group (330 ms) in panel **C**.

148 ± 8 ms by Noda et al.[13] It was longer than that in the idiopathic VF of Purkinje origin reported by Haissaguerre et al[11] (145 ± 12 vs. 126 ± 18 ms; $P = .04$) and also slightly but significantly longer than that in the benign form of RVOT VT reported by Noda et al[13] (148 ± 8 vs. 142 ± 12 ms; $P = .03$).

On the other hand, Noda et al[13] suggested a significant difference of the cycle length (CL) of VT between malignant and benign forms of RVOT VT (245 ± 28 vs. 328 ± 65 ms; $P<.0001$)[13] (Table 1); however, it was not surprising that the CL of polymorphic VT in the malignant group was shorter than that of monomorphic VT in the benign group. Therefore, we further analyzed the CL of monomorphic VT between malignant and benign groups. Among 16 patients with the malignant form of RVOT VT, both monomorphic RVOT VT and polymorphic RVOT VT were recorded in seven patients. The CL of monomorphic VT recorded in the seven malignant RVOT VT group patients was still significantly shorter than the CL of monomorphic VT in the 85 benign RVOT VT group patients (273 ± 23 vs. 328 ± 65 ms; $P = .0001$; Figure 2). Among the seven malignant RVOT VT group patients, the CL of monomorphic VT tended to be longer than that of polymorphic VT (273 ± 23 vs. 241 ± 36 ms; $P = .08$). Moreover, a previous history of syncope with malignant characteristics was more frequently observed in the seven malignant RVOT VT group patients than in the 85 benign RVOT VT group patients (5/7 vs. 15/85; $P = .005$). These data suggest that a shorter CL during monomorphic VT, when present, as well as a history of syncope with malignant characteristics, may be a predictor of the coexistence of malignant VF or polymorphic VT in patients with idiopathic VT originating from RVOT. In consideration of the available evidence, Holter or monitor ECG to record spontaneous episodes of RVOT VT and obtaining detailed previous history of syncope with malignant characteristics are useful to differentiate the malignant form from the benign form of RVOT VT.

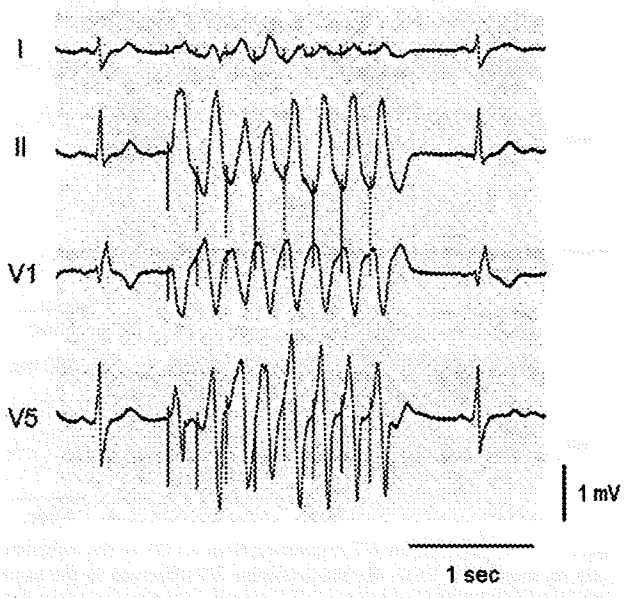

Figure 3 Polymorphic changes of the QRS complex on ECG leads I, II, V1, and V5 during rapid pacing in a patient with the malignant form of idiopathic VT originating from RVOT. The morphological changes were induced by rapid pacing from the origin of the initiating VPC, which was confirmed by the efficacy of radiofrequency catheter ablation. Reproduced from reference 13 with permission.

Possible mechanism of the malignant form of idiopathic VT originating from RVOT

Although the mechanism of benign idiopathic monomorphic VT arising from RVOT is considered to be triggered activity,[2] that of the malignant form of idiopathic RVOT VT is unknown because of less investigation of electrophysiologic characteristics during the ablation procedure. Among the 16 patients with malignant idiopathic RVOT VT reported by Noda and coworkers,[13] programmed electrical stimulations induced VF in one patient and polymorphic VT in two patients. We also conducted rapid pacing from the origin of initiating VPCs after radiofrequency catheter ablation and could reproduce polymorphic morphological changes in the QRS configuration in two of seven patients[13] (Figure 3). It is speculated that functional block and/or delayed conduction by rapid firing due to triggered activity or microreentry arising from a single focus led to chaotic ventricular conduction, thus causing VF and/or polymorphic VT. However, it is also speculated that rapid firing from close multiple foci one after another produces polymorphic morphological changes in the QRS configuration, since other VPCs with slightly different QRS morphology often appeared after eliminating the initial target VPCs by radiofrequency ablation.

Therapy and follow-up

Similar to the benign form of idiopathic VT originating from RVOT, radiofrequency catheter ablation was conducted to prevent VF or polymorphic VT in patients with the malignant form of idiopathic RVOT VT.[11] Precise mapping and catheter ablation for the malignant form of RVOT VT require a clear-cut trigger in the form of frequent VPCs, just as for the benign form of RVOT VT. Haissaguerre et al[11] performed catheter ablation in four patients with idiopathic VF elicited from RVOT. Late recurrence of VPCs with the same morphology as preablation was observed in one patient; however, sudden cardiac death, syncope, or recurrence of VF were not reported. In the three patients with the malignant form of idiopathic RVOT VT reported by Viskin et al,[12] radiofrequency catheter ablation was conducted in only one patient, an implantable defibrillator-cardioverter (ICD) was implanted in the remaining two patients, and all three patients were reported to be free of arrhythmia recurrence. Noda et al[13] performed radiofrequency catheter ablation in all 16 patients with the malignant form of idiopathic VT arising from RVOT. The ICD was implanted in one patient with induced VF after ablation, and β-blocker was used in four patients with partially successful ablation. During 106 months of follow-up, no recurrence of syncope, VF, or cardiac arrest was observed. How-

ever, among our series of the 16 patients with malignant idiopathic RVOT VT, a significant sign of ARVD (aneurysmal formation of the RV mid to apex, dilatation of the RVOT) was developed in one patient 10 years later after catheter ablation. These data suggest that radiofrequency catheter ablation seems to be effective to cure the malignant form of idiopathic VT arising from RVOT; however, a backup of ICD implantation is required in patients with the malignant form of idiopathic RVOT VT, especially in those with documented VF or cardiac arrest, since the feasibility of ablation has been demonstrated in small series of patients in expert centers and long-term follow-up data of catheter ablation are lacking. Moreover, our data indicate that careful morphological follow-up with cardiac imaging is also needed for early detection of progression to ARVD in some patients with the malignant form of benign-looking RVOT VT.

Acknowledgment

The author thanks Takashi Noda in the Division of Cardiology, Department of Internal Medicine, National Cardiovascular Center, for providing ECG recordings.

References

1. Zipes DP, Camm AJ, Borggrefe M, et al. ACC/AHA/ESC 2006 guidelines for management of patients with ventricular arrhythmias and the prevention of sudden cardiac death: a report of the American College of Cardiology/American Heart Association Task Force and the European Society of Cardiology Committee for Practice Guidelines. J Am Coll Cardiol 2006;48:e247–e346.
2. Stevenson WG, Soejima K. Catheter ablation for ventricular tachycardia. Circulation 2007;115:2750–2760.
3. Corrado D, Basso C, Leoni L, et al. Three-dimensional electroanatomical voltage mapping and histologic evaluation of myocardial substrate in right ventricular outflow tract tachycardia. J Am Coll Cardiol 2008;51:731–739.
4. Dalal D, Tandri H, Judge DP, et al. Morphologic variants of familial arrhythmogenic right ventricular dysplasia/cardiomyopathy a genetics-magnetic resonance imaging correlation study. J Am Coll Cardiol 2009;53:1289–1299.
5. O'Donnell D, Cox D, Bourke J, Mitchell L, Furniss S. Clinical and electrophysiological differences between patients with arrhythmogenic right ventricular dysplasia and right ventricular outflow tract tachycardia. Eur Heart J 2003;24:801–810.
6. Vestal M, Wen MS, Yeh SJ, Wang CC, Lin FC, Wu D. Electrocardiographic predictors of failure and recurrence in patients with idiopathic right ventricular outflow tract tachycardia and ectopy who underwent radiofrequency catheter ablation. J Electrocardiol 2003;36:327–332.
7. Krittayaphong R, Sriratanasathavorn C, Dumavibhat C, et al. Electrocardiographic predictors of long-term outcomes after radiofrequency ablation in patients with right-ventricular outflow tract tachycardia. Europace 2006;8:601–606.
8. Tanner H, Hindricks G, Schirdewahn P, et al. Outflow tract tachycardia with R/S transition in lead V3: six different anatomic approaches for successful ablation. J Am Coll Cardiol 2005;45:418–423.
9. Dixit S, Gerstenfeld EP, Callans DJ, Marchlinski FE. Electrocardiographic patterns of superior right ventricular outflow tract tachycardias: distinguishing septal and free-wall sites of origin. J Cardiovasc Electrophysiol 2003;14:1–7.
10. Iwai S, Cantillon DJ, Kim RJ, et al. Right and left ventricular outflow tract tachycardias: evidence for a common electrophysiologic mechanism. J Cardiovasc Electrophysiol 2006;17:1052–1058.
11. Haissaguerre M, Shoda M, Jais P, et al. Mapping and ablation of idiopathic ventricular fibrillation. Circulation 2002;106:962–967.
12. Viskin S, Rosso R, Rogowski O, Belhassen B. The "short-coupled" variant of right ventricular outflow ventricular tachycardia: a not-so-benign form of benign ventricular tachycardia? J Cardiovasc Electrophysiol 2005;16:912–916.
13. Noda T, Shimizu W, Taguchi A, et al. Malignant entity of idiopathic ventricular fibrillation and polymorphic ventricular tachycardia initiated by premature extrasystoles originating from right ventricular outflow tract. J Am Coll Cardiol 2005;46:1288–1294.
14. Wright M, Sacher F, Haïssaguerre M. Catheter ablation for patients with ventricular fibrillation. Curr Opin Cardiol 2009;24:56–60.
15. Viskin S, Belhassen B. Idiopathic ventricular fibrillation. Am Heart J 1990;120:661–671.
16. Leenhardt A, Glaser E, Burguera M, Nurnberg M, Maison-Blanche P, Coumel P. Short-coupled variant of torsade de pointes. A new electrocardiographic entity in the spectrum of idiopathic ventricular tachyarrhythmias. Circulation 1994;89:206–215.
17. Betts TR, Yue A, Roberts PR, Morgan JM. Radiofrequency ablation of idiopathic ventricular fibrillation guided by noncontact mapping. J Cardiovasc Electrophysiol 2004;15:957–959.
18. Kataoka M, Takatsuki S, Tanimoto K, et al. A case of vagally mediated idiopathic ventricular fibrillation. Nat Clin Pract Cardiovasc Med 2008;5:111–115.
19. Naik N, Juneja R, Sharma G, Yadav R, Anandraja S. Malignant idiopathic ventricular fibrillation "cured" by radiofrequency ablation. J Interv Card Electrophysiol 2008;23:143–148.

An international compendium of mutations in the *SCN5A*-encoded cardiac sodium channel in patients referred for Brugada syndrome genetic testing

Jamie D. Kapplinger, BA,* David J. Tester, BS,* Marielle Alders, PhD,† Begoña Benito, MD,‡ Myriam Berthet, BA,§‖ Josep Brugada, MD, PhD,¶ Pedro Brugada, MD, PhD,# Véronique Fressart, MD,§‖** Alejandra Guerchicoff, PhD,†† Carole Harris-Kerr, PhD,‡‡ Shiro Kamakura, MD, PhD,§§ Florence Kyndt, PhD,‖‖¶¶## Tamara T. Koopmann, PhD,*** Yoshihiro Miyamoto, MD,††† Ryan Pfeiffer, BS,†† Guido D. Pollevick, PhD,‡‡ Vincent Probst, MD, PhD,‖‖## Sven Zumhagen, MD,‡‡‡ Matteo Vatta, PhD,§§§ Jeffrey A. Towbin, MD,‖‖‖ Wataru Shimizu, MD, PhD,§§ Eric Schulze-Bahr, MD,‡‡‡ Charles Antzelevitch, PhD,†† Benjamin A. Salisbury, PhD,‡‡ Pascale Guicheney, PhD,§‖** Arthur A. M. Wilde, MD, PhD,*** Ramon Brugada, MD, PhD,¶¶¶ Jean-Jacques Schott, PhD,‖‖¶¶### Michael J. Ackerman, MD, PhD*

*From the *Departments of Medicine, Pediatrics, and Molecular Pharmacology and Experimental Therapeutics/Divisions of Cardiovascular Diseases and Pediatric Cardiology, Windland Smith Rice Sudden Death Genomics Laboratory, Mayo Clinic, Rochester, Minnesota, †Department of Clinical Genetics, Academic Medical Centre, Amsterdam, the Netherlands, ‡Departamento de Biotecnología, Universidad Politécnica de Madrid, Madrid, Spain, §Inserm, U956, Groupe Hospitalier Pitié-Salpêtrière, Paris, France, ‖UPMC Univ Paris 06, UMR-S956, IFR14, Paris, France, ¶Hospital Clínic, University of Barcelona, Barcelona, Spain, #Heart Rhythm Management Centre, Cardiovascular Institute, UZ Brussel, VUB Brussels, Brussels, Belgium, **AP-HP, Groupe Hospitalier Pitié-Salpêtrière, Service de Biochimie, Unité de Cardiogénétique et Myogénétique, Paris, France, ††Masonic Medical Research Laboratory, Utica, New York, ‡‡PGxHealth, LLC, a division of Clinical Data, Inc., New Haven, Connecticut, §§Division of Cardiology, Department of Internal Medicine, National Cardiovascular Center, Suita, Japan, ‖‖Institut National de la Sante et de la Recherche Medicale, UMR 915, F-44000 Nantes, France, ¶¶CNRS ERL3147, F-44000 Nantes, France, ##Service de Cardiologie, L'Institut du Thorax Centre Hospitalier Universitaire de Nantes, F-44000 Nantes, France, ***Heart Failure Research Centre, Department of Cardiology, Academic Medical Centre, Amsterdam, the Netherlands, †††Laboratory of Molecular Genetics, National Cardiovascular Center, Suita, Japan, ‡‡‡Genetics of Heart Diseases, Hospital of the University of Münster, Germany, §§§Department of Pediatrics (Cardiology) and Department of Molecular Physiology and Biophysics, Baylor College of Medicine, Houston, Texas, ‖‖‖The Heart Institute, Cincinnati Children's Hospital Medical Center, Cincinnati, Ohio, ¶¶¶Cardiovascular Genetics Center, School of Medicine, University of Girona, Spain, and ###Faculté de Médecine, L'Institut du Thorax, Université de Nantes, F-44000 Nantes, France.*

Support for data analysis for this project was provided by the Mayo Clinic Windland Smith Rice Comprehensive Sudden Cardiac Death Program (Dr. Ackerman), grant HL47678 from the National Institutes of Health (Dr. Antzelevitch), New York State and Florida Free and Accepted Masons, the GIS Institut des Maladies Rares, the AFM (ANR-06-MRAR-022, PG, Dr. Schott), The Health Sciences Research Grants (H18, Research on Human Genome, 002) and the Research Grant for the Cardiovascular Diseases (21C-8) from the Ministry of Health, Labor, and Welfare of Japan (Dr. Shimizu), The Fondation Leducq Trans-Atlantic Network of Excellence Grant (05 CVD 01, Preventing Sudden Death, Dr. Schott), ANR grant ANR/-05-MRAR-028-01 (Dr. Schott), grant from the Fondation pour la recherche Medicale (Dr. Schott), FIS-ISCiii (Dr. Brugada), CNIC (Dr. Brugada), Ramon Brugada Sr. Foundation (Dr. Brugada), Leducq Foundation, grant 05 CVD, Alliance against Sudden Cardiac death (Drs. Wilde, Schott, and Schulze-Bahr), and Deutsche Forschungsgemeinschaft (Dr. Schulze-Bahr). All mutational analyses performed in this study were conducted at individual centers. Dr. Ackerman is a consultant for PGxHealth. Intellectual property derived from Dr. Ackerman's research program resulted in license agreements in 2004 between Mayo Clinic Health Solutions (formerly Mayo Medical Ventures) and PGxHealth (formerly Genaissance Pharmaceuticals). Mr. Kapplinger and Mr. Tester contributed equally to this work. **Address reprint requests and correspondence:** Dr. Michael J. Ackerman, Windland Smith Rice Sudden Death Genomics Laboratory, Guggenheim 501, Mayo Clinic, Rochester, Minnesota 55905. E-mail address: ackerman.michael@mayo.edu. (Received August 26, 2009; accepted September 25, 2009.)

1547-5271/$ -see front matter doi:10.1016/j.hrthm.2009.09.069

BACKGROUND Brugada syndrome (BrS) is a common heritable channelopathy. Mutations in the *SCN5A*-encoded sodium channel (BrS1) culminate in the most common genotype.

OBJECTIVE This study sought to perform a retrospective analysis of BrS databases from 9 centers that have each genotyped >100 unrelated cases of suspected BrS.

METHODS Mutational analysis of all 27 translated exons in *SCN5A* was performed. Mutation frequency, type, and localization were compared among cases and 1,300 ostensibly healthy volunteers including 649 white subjects and 651 nonwhite subjects (blacks, Asians, Hispanics, and others) that were genotyped previously.

RESULTS A total of 2,111 unrelated patients (78% male, mean age 39 ± 15 years) were referred for BrS genetic testing. Rare mutations/variants were more common among BrS cases than control subjects (438/2,111, 21% vs. 11/649, 1.7% white subjects and 31/651, 4.8% nonwhite subjects, respectively, $P < 10^{-53}$). The yield of BrS1 genetic testing ranged from 11% to 28% ($P = .0017$). Overall, 293 distinct mutations were identified in *SCN5A:* 193 missense, 32 nonsense, 38 frameshift, 21 splice-site, and 9 in-frame deletions/insertions. The 4 most frequent BrS1-associated mutations were E1784K (14×), F861WfsX90 (11×), D356N (8×), and G1408R (7×). Most mutations localized to the transmembrane-spanning regions.

CONCLUSION This international consortium of BrS genetic testing centers has added 200 new BrS1-associated mutations to the public domain. Overall, 21% of BrS probands have mutations in *SCN5A* compared to the 2% to 5% background rate of rare variants reported in healthy control subjects. Additional studies drawing on the data presented here may help further distinguish pathogenic mutations from similarly rare but otherwise innocuous ones found in cases.

KEYWORDS Brugada syndrome; Genetic testing; Ion channels; Sodium channel; Sudden death

ABBREVIATIONS **BrS** = Brugada syndrome; **BrS1** = Brugada syndrome type 1; **ChIPs** = sodium channel interacting proteins; **ECG** = electrocardiographic; **IDL** = interdomain linker; I_{Na} = available sodium current; **LQT3** = long-QT syndrome type 3; **LQTS** = long-QT syndrome; **MAF** = minor allele frequency; **PCR** = polymerase chain reaction; **SCD** = sudden cardiac death

(Heart Rhythm 2010;7:33–46)

Introduction

Brugada syndrome (BrS) is a rare heritable arrhythmia syndrome characterized by an electrocardiographic (ECG) pattern consisting of coved-type ST-segment elevation in the right precordial leads V_1 through V_3 (often referred to as a type-1 Brugada ECG pattern) and an increased risk for sudden cardiac death (SCD).[1,2] The penetrance and expressivity of this autosomal-dominant disorder is highly variable, ranging from a lifelong asymptomatic course to SCD during the first year of life. The syndrome is thought to account for up to 4% of all SCDs and 20% of unexplained sudden death in the setting of a structurally normal heart;[3] however, some patients display a more benign course. BrS is generally considered a disorder involving young male adults, with arrhythmogenic manifestation first occurring at an average age of 40 years, with sudden death typically occurring during sleep.[4] However, BrS has also been demonstrated in children and infants as young as 2 days old and may serve as a pathogenic basis for some cases of sudden infant death syndrome.[3]

Since the disorder's sentinel clinical and ECG description in 1992 by Drs. Pedro and Josep Brugada,[5] *SCN5A*-encoded cardiac sodium channel loss-of-function mutations have been shown to confer the pathogenic basis for an estimated 15% to 30% of BrS, currently representing the most common BrS genotype and classified as Brugada syndrome type 1 (BrS1).[6–8] Loss-of-function mutations in *SCN5A* reduce the overall available sodium current (I_{Na}) through either impaired intracellular trafficking of the ion channel to the plasma membrane, thereby reducing membrane surface channel expression, or through altered gating properties of the channel. Gain-of-function *SCN5A* mutations cause a clinically and mechanistically distinct arrhythmia syndrome, long-QT syndrome type 3 (LQT3). Interestingly, some identical *SCN5A* mutations may provide either a loss-of-function BrS1-phenotype or a gain-of-function LQT3-phenotype, depending on the individual host. In fact, LQT3/BrS/conduction-disorder *SCN5A* overlap syndromes do exist within single large families.[9,10]

After a decade of genetic testing by research laboratories worldwide, BrS genetic testing has made the transition from discovery to translation to clinical implementation with the availability of clinical BrS1 genetic testing (since 2004 in North America and even earlier in Europe), which provides comprehensive open-reading frame and canonical splice site mutational analysis of *SCN5A*. However, it must be recognized that nearly 2% of healthy Caucasians and 5% of healthy nonwhite subjects also host rare missense *SCN5A* variants, leading to a potential conundrum in the interpretation of the genetic test results.[11] Distinguishing pathogenic mutations from rare harmless genetic variants is of critical importance in the interpretation of genetic testing and the management of genotype-positive BrS patients.

Presently, there are over 100 BrS1-associated mutations publicly available (http://www.fsm.it/cardmoc). We sought to assemble an international compendium of putative BrS1-associated mutations through a retrospective analysis of BrS genomic databases from 9 reference centers throughout the world (5 Europe, 3 United States, 1 Japan) that have each genotyped >100 unrelated cases of clinically suspected BrS. Such a compendium may illuminate further key structure–function properties and provide a foundational building block for the development of algorithms to assist in distinguishing pathogenic mutations from similarly rare but otherwise innocuous ones.

Methods

Study population

A retrospective analysis of BrS databases from 9 centers throughout the world that have each genotyped >100 unrelated cases of clinically suspected BrS was performed. In total, 2,111 unrelated patients (78% male, mean age 39 ±

Table 1 Demographics and mutation yield for 9 Brugada syndrome genetic testing centers

	1	2	3	4	5	6	7	8	9
Total	451	365	311	237	195	158	153	130	111
Positive	92	88	69	50	44	26	43	14	12
Age (yrs)	47 ± 14	40 ± 11	45 ± 18	43 ± 14	35 ± 18	36 ± 21	45 ± 15	48 ± 10	37 ± 21
Range (yrs)	3 to 70	0 to 77	0 to 82	8 to 80	0 to 76	0 to 69	5 to 65	28 to 64	7 to 78
Yield (%)	20.4	24.1	22.2	21.1	22.6	16.5	28.1	10.8	10.8
Male	357	277	239	193	140	117	106	124	72
Positive	68	67	55	40	31	17	30	13	7
Yield (%)	21.6	24.2	22.2	20.7	23.4	14.5	28.3	10.5	9.7
Female	94	88	72	44	55	41	47	6	39
Positive	23	19	14	10	13	9	13	1	5
Yield (%)	25.5	21.6	19.4	22.7	23.6	22.0	27.7	16.7	12.8

Center: 1 = Nantes, 2 = Brugada, 3 = AMC, 4 = Paris, 5 = PGxHealth, 6 = MMRL, 7 = UKM, 8 = NCVC, 9 = BCM.

15 years) were referred for *SCN5A* genetic testing (Table 1). For the purpose of this compendium of identified mutations, only minimal demographic information for each center's cohort, such as the average age and range of age at diagnosis and the number of male and female subjects was provided. The specific age and gender were collected for mutation-positive patients. A sample was accepted for genetic testing if the referring physician had made a clinical diagnosis of either possible or definite BrS. An ECG was not always available for each patient. Although DNA samples were accepted for analysis based on a referral diagnosis of BrS, several of the international centers did collect and examine 12-lead ECGs to confirm the presence of an ECG pattern consistent with BrS.

Mutational analysis

Patient genomic DNA was analyzed for mutations in all 27 translated exons, including splice sites and adjacent regions, of the *SCN5A*-encoded cardiac sodium channel $Na_V1.5$ using a combination of polymerase chain reaction (PCR), either denaturing high-performance liquid chromatography or single-stranded conformation polymorphism and DNA sequencing.[12] In addition, frequency, location, and mutation type of *SCN5A* genetic variation found among 1,300 ostensibly healthy volunteers,[11,13] including 649 white subjects and 651 nonwhite subjects (black, Asian, and Hispanic), was analyzed and compared with the possible BrS1-associated mutations. To be reported in this compendium as a possible BrS1-associated mutation, the case mutation must have been absent among all 1,300 control subjects who underwent comprehensive mutation scanning. Further, each reference center examined a local set of control samples from usually 200 to 400 additional unrelated, healthy individuals to determine the presence or absence of each possible case mutation observed in patients from their respective geographical region.

Mutation nomenclature

All possible BrS1-associated mutations were denoted using the accepted Human Genome Variation Society's guidelines for nomenclature.[14] The nucleotide and amino acid designations were based on the *SCN5A* transcript NM_198056.2. For example, the missense mutation E1784K would indicate the wild-type amino acid (E = glutamic acid) at position 1784 is replaced by lysine (K). Frameshift mutations resulting from nucleotide insertions or deletions were annotated using the F861WfsX90 format, which indicates that the wild-type phenylalanine (F) at position 861 is altered to a tryptophan (W) followed by 89 miscoded amino acids prior to a termination codon (X) 90 residues from the beginning of the altered reading frame.

A substitution of either the first or the last 2 nucleotides of a particular exon has the capacity to alter proper mRNA splicing, regardless of whether the nucleotide substitution codes for a different amino acid (missense mutation) produces a stop codon (nonsense mutation) or does not alter the open reading frame at all (i.e., a synonymous or silent single-nucleotide substitution).[15–17] As such, mutations involving this exonic portion of the splice site were considered as possible splicing mutations in this study and annotated as either missense/splice-site, nonsense/splice-site, or silent/splice-site mutations to distinguish them from intronic mutations predicted to disrupt splicing.

Topological placement of the mutations was assigned using a combination of Swissprot (http://ca.expasy.org/uniprot/) and recent studies of the linear topologies for the sodium channel pore-forming alpha subunit.[18–20] The Swissprot database provides generally accepted residue ranges corresponding with each ion-channel region and specialized subregions. For Nav1.5, mutations were localized to either the N-terminus (amino acids 1 to 126), interdomain linker (IDL I-II, aa 416-711, IDL II-III, aa 940-1200, and IDL III-IV, aa 1471-1523), transmembrane/linker (Domain I, aa 127-415, Domain II, aa 712-939, Domain III, aa 1201-1470, Domain IV, aa 1524-1772), or C-terminus (aa 1773-2016). The transmembrane-spanning region was further subdivided into S1 through S4 (DI S1-S4/S5, aa 127-252, DII S1-S4/S5, aa 712-841, DIII S1-S4/S5, aa 1201-1336, and DIV S1-S4/S5, aa 1524-1659) and S5 through S6, the pore region and selectivity filter of the channel (DI S5-S6, aa 253-415, DII S5-S6, aa 842-939, DIII S5-S6, aa 1337-1470, DIV S5-S6, aa 1660-1772).

Defining terminology: variant versus mutation

For the purposes of this compendium, a variant will be defined as any change to the wild-type sequence, whether it is in case or control subjects. Mutations will be identified as rare, case-only (absent in the 1,300+ healthy volunteers) variants that are possibly pathogenic. Variants identified with a minor allele frequency (MAF) >0.5% among the 1,300 healthy control subjects will be termed common polymorphisms. If the MAF is <0.5%, these variants will be termed uncommon/rare polymorphisms.

Defining a variant as a possible BrS1-causative mutation

To be considered as a possible BrS1-causing mutation, the variant must disrupt either the open reading frame (i.e., missense, nonsense, insertion/deletion, or frameshift mutations) or the splice site (polypyrimidine tract, splice acceptor, or splice donor recognition sequences). In addition to the exonic splice sites described above, the acceptor splice site was defined as the 3 intronic nucleotides preceding an exon (designated as IVS-1, -2, or -3) and the donor splice site as the first 5 intronic nucleotides after an exon (designated as IVS+1, +2, +3, +4, or +5).[17] Additionally, single-nucleotide substitutions (namely, a purine [A or G] for a pyrimidine [C or T]) within the polypyrimidine tract immediately preceding the acceptor splice-site may be causative.[17] As such, some pyrimidine-to-purine substitutions in this region of the intron have been included as potentially pathogenic. For example, an IVS-5 cytosine (C) that falls within the polypyrimidine tract and is substituted by an adenine (A) that would predictably disrupt the polypyrimidine tract and consequently result in aberrant splicing would be included as a possible pathogenic mutation. Hence, single-nucleotide substitutions that obviously did not change the open reading frame (i.e., synonymous single-nucleotide polymorphisms) or those outside of the splice site recognition sequence were not included in either case or control subjects for this study.

Additionally, to be considered as a possible BrS1-causing mutation, the nonsynonymous variant must have been absent in all published databases listing the *SCN5A* channel common polymorphisms and previously published reports or compendia of rare control variants, e.g., those found in over 2,600 reference alleles (Table 2) derived from over 1,300 ostensibly healthy adult volunteers.[11,13] As such, the sole or concomitant presence of a common polymorphism such as H558R-SCN5A or a rarer polymorphism such as A572D-SCN5A would not by definition warrant the annotation of possible BrS1-associated mutation and would not be counted toward the assignment of compound or multiple mutation status to an individual in this compendium. This does not imply that common and rare polymorphisms may not possibly modulate the BrS1 phenotype.

Results

Overall, 2,111 unrelated patients (78% male, average age at testing 39 ± 15 years) were referred for BrS genetic testing across 9 testing centers (Table 1). As expected, rare *SCN5A* missense mutations were far more common among BrS cases (438/2,111, 21%) than similarly rare genetic variants were among control subjects (43/1,300 [11/649, 1.7% white subjects and 31/651, 4.8% nonwhite subjects], $P < 10^{-55}$). The yield differed significantly across centers ($P = .0017$; $chi^2 = 24.7$, degrees of freedom (df) = 8), ranging from 11% (centers 8 [14/130] and 9 [12/111]) to 28% (center 7 [43/153], $P = .0017$ for the 9 centers) (Table 1, Figure 1). There was no significant difference in yield between male (324/1,520, 21.3%) and female (112/439, 25.5%, $P = .07$) subjects. Of the 438 *SCN5A* mutation-positive cases, 13 (3%) harbored multiple mutations (Table 3). All 13 were male and trended toward younger age at diagnosis (29.7 ± 16.2 years) than male subjects with a single mutation (39.2 ± 14.4 years, $P = .07$).

Overall, 293 distinct, possible BrS1-associated mutations (200, 68% novel to this cohort), absent in 2,600 reference alleles, were identified in the 438 genotype-positive cases, 225 (77%) of which were identified only once (Table 4, Figure 2). Only 68 mutations were found in multiple unrelated patients. The 4 most frequent BrS1-associated mutations were E1784K (14 patients), F861WfsX90 (11 patients), D356N (8 patients), and G1408R (7 patients) (Table 4, Figure 2). Two-thirds of the unique mutations were missense mutations (193), whereas the remaining third (100) involved radical mutations (38 frameshift, 32 nonsense, 21 splice-site, and 9 in-frame insertions or deletions) (Table 4, Figure 3).

Of the 293 unique mutations, 208 (71%) localized to one of the 4 transmembrane-spanning regions (DI, DII, DIII, or DIV), 54 (18%) localized to an IDL (31 in IDL I-II, 17 in IDL II-III, and 6 in IDL III-IV), 17 (6%) localized to the C-terminus, and 14 (5%) localized to the N-terminus (Table 4, Figure 4). The majority of patients with a single *SCN5A* mutation (313/425, 74%) hosted a mutation that localized to the transmembrane region of the channel, with 31% (133/425) having a mutation that localized to either DI S1-S4, DII S1-S4, DIII S1-S4, or DIV S1-S4 and 42% (180/425) having a mutation that localized to the S5, P-loop, and S6 regions containing the pore and selectivity filter of the sodium channel (DI S5-S6, DII S5-S6, DIII S5-S6, or DIV S5-S6) (Table 4, Figure 4). In fact, compared with the topological location for the rare control variants, there was a strong predilection for a patient's possible BrS1-associated mutation to localize to the channel's transmembrane (S1-S4 6.3% vs. 0.2%, $P < 10^{-24}$) and pore-forming segments (S5-S6 8.5% vs. 0.5%, $P < 10^{-30}$) (Figure 5). Twenty-eight patients (1.3%) had their possible BrS1-associated missense mutation localizing to the DI-DII or DII-DIII linker domains, where the vast majority of the rare missense SCN5A variants, which were discovered among the ostensibly healthy control subjects, reside. The yield for the linker regions was 3% for cases compared with 1.7% for healthy subjects (P = NS) (Figure 5).

Interestingly, 10 (3.4%) of the mutations, identified in 29 patients of this BrS compendium, have been identified previously in cases of long-QT syndrome (LQTS): G615E, L619F, E1225K, P1332L, L1501V, R1623Q, I1660V, V1667I, T1779M, including the most common BrS1-associated muta-

Table 2 Control variants found in 2,600 reference alleles

Exon	Nucleotide change	Variant	Mutation type	Location	Number	Ethnicity	Status
2	52 C>T	R18W	Missense	N-terminal	1	O	Rare control
2	100 C>T	R34C	Missense	N-terminal	44	B>H=O>W>A	Polymorphism
2	101 G>A	R34H	Missense	N-terminal	1	B	Rare control
6	647 C>T	S216L	Missense	DI-S3/S4	4	W	Polymorphism
7	856 G>T	A286S	Missense	DI-S5/S6	1	B	Rare control
7	872 A>G	N291S	Missense	DI-S5/S6	1	O	Rare control
7	895 T>A	L299M	Missense	DI-S5/S6	1	B	Rare control
9	1126 C>T	R376C	Missense	DI-S5/S6	1	W	Rare control
11	1340 C>G	A447G	Missense	DI/DII	1	B	Rare control
11	1345 A>G	T449A	Missense	DI/DII	1	O	Rare control
11	1381 T>G	L461V	Missense	DI/DII	2	B	Polymorphism
11	1425 A>C	R475S	Missense	DI/DII	1	B	Rare control
11	1441 C>T	R481W	Missense	DI/DII	6	B>H=O	Polymorphism
12	1571 C>A	S524Y	Missense	DI/DII	18	B>W=H	Polymorphism
12	1673 A>G	H558R	Missense	DI/DII	408	W>B>H>O>A	Polymorphism
12	1703 G>A	R568H	Missense	DI/DII	1	W	Rare control
12	1735 G>A	G579R	Missense	DI/DII	1	W	Rare control
12	1776 C>A	N592K	Missense	DI/DII	1	W	Rare control
12	1787 A>G	D596G	Missense	DI/DII	1	B	Rare control
12	1802 T>C	V601A	Missense	DI/DII	1	W	Rare control
12	1852 C>T	L618F	Missense	DI/DII	1	O	Rare control
13	1913 G>A	G638D	Missense	DI/DII	1	A	Rare control
13	1967 C>T	P656L	Missense	DI/DII	1	B	Rare control
13	2014 G>A	A672T	Missense	DI/DII	1	A	Rare control
14	2066 G>A	R689H	Missense	DI/DII	1	H	Rare control
14	2074 C>A	Q692K	Missense	DI/DII	3	W	Polymorphism
14	2114 C>T	S705F	Missense	DI/DII	1	A	Rare control
16	2770 G>A	V924I	Missense	DII-S6	2	B=O	Polymorphism
17	2924 C>T	R975W	Missense	DII/DIII	1	W	Rare control
17	2957 G>A	R986Q	Missense	DII/DIII	1	B	Rare control
17	3047 C>T	T1016M	Missense	DII/DIII	1	A	Rare control
17	3118 G>A	G1040R	Missense	DII/DIII	1	B	Rare control
18	3245 T>C	V1082A	Missense	DII/DIII	1	B	Rare control
18	3269 C>T	P1090L	Missense	DII/DIII	5	A>W	Polymorphism
18	3292 G>T	V1098L	Missense	DII/DIII	1	A	Rare control
18	3308 C>A	S1103Y	Missense	DII/DIII	31	B>O>H	Polymorphism
18	3319 G>A	E1107K	Missense	DII/DIII	1	A	Rare control
18	3346 C>T	R1116W	Missense	DII/DIII	2	A	Polymorphism
20	3578 G>A	R1193Q	Missense	DII/DIII	12	A>W	Polymorphism
21	3751 G>A	V1251M	Missense	DIII-S2	1	B	Rare control
22	3878 T>C	F1293S	Missense	DIII-S3/S4	2	W	Polymorphism
22	3922 C>T	L1308F	Missense	DIII-S4	3	O>B	Polymorphism
Intron 24	4299 +2 T>A	1433sp	Splice site	DIII-S5/S6	1	W	Rare control
26	4534 C>T	R1512W	Missense	DIII/DIV	1	H	Rare control
28	5360 G>A	S1787N	Missense	C-terminal	3	W	Polymorphism
28	5507 T>C	I1836T	Missense	C-terminal	1	B	Rare control
28	5701 G>A	E1901K	Missense	C-terminal	1	W	Rare control
28	5755 C>T	R1919C	Missense	C-terminal	1	B	Rare control
28	5851 G>T	V1951L	Missense	C-terminal	16	H>A>B=O	Polymorphism
28	5873 G>A	R1958Q	Missense	C-terminal	1	B	Rare control
28	5885 C>T	P1962L	Missense	C-terminal	1	B	Rare control
28	5904 C>G	I1968M	Missense	C-terminal	1	B	Rare control
28	5972 G>A	R1991Q	Missense	C-terminal	1	B	Rare control
28	6010 T>C	F2004L	Missense	C-terminal	7	W>H	Polymorphism
28	6016 C>G	P2006A	Missense	C-terminal	3	W>B	Polymorphism

The > and = symbols represent the relative prevalence of the variant of interest in each corresponding ethnicity.
A = Asian; B = black; H = Hispanic; O = other; and W = white.

tion, E1784K, observed in this BrS compendium. Five of the 10 have been functionally characterized previously, with L619F,[21] P1332L,[22] R1623Q,[23] and E1784K[24] producing channel abnormalities consistent with an LQT3 phenotype and G615E[25] producing a wild-type–like SCN5A channel.[10]

Discussion

Since the first report by Chen et al[26] in 1998, a little over 100 unique *SCN5A* mutations have been implicated as possibly causative for BrS1. Previous small cohort studies have indicated that the prevalence of *SCN5A* mutations in BrS is

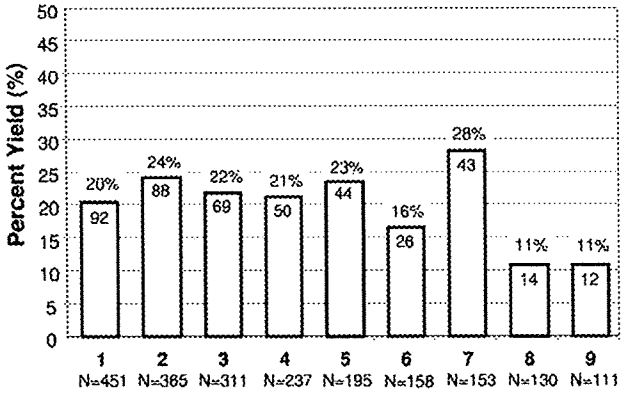

Figure 1 Mutation detection yield by genetic testing center. Depicted here is a comparison of Brugada syndrome genetic testing for each of the 9 centers ordered according to the total number (N = X) of unrelated patients tested. The number within each column represents the number of genotype positive patients for the respective center. For example, Center 1 analyzed 451 unrelated cases and identified a putative pathogenic mutation in 92 (20%). Center: 1 = Nantes, 2 = Brugada, 3 = AMC, 4 = Paris, 5 = PGxHealth, 6 = MMRL, 7 = UKM, 8 = NCVC, 9 = BCM.

roughly 15% to 20%, and possibly as high as 40% in cases of familial BrS. In 2000, Priori et al[6] reported a 15% yield with respect to *SCN5A* mutations among 52 unrelated patients. In 2002, these investigators extended their analysis to 130 probands (20% with a family history of sudden unexplained death) and identified an *SCN5A* mutation in 22%.[7] Schulze-Bahr et al[8] reported a 14% yield among 44 unrelated BrS patients, who are included in the current compendium.

Here, through this international multicenter study, we provide an expanded compendium of 293 unique (200 novel) BrS1-associated *SCN5A* mutations derived from over 2,100 unrelated patients referred for BrS genetic testing. The overall yield was 21% and ranged from 11% to 28% among the 9 centers. The differences in yield between the centers may be due to technical differences in mutational analysis methods used among laboratories, but it more likely reflects phenotypic differences among cohorts. For example, the cohorts with the lowest yield may have a preponderance of sporadic cases compared with familial cases. In 2003, Schulze-Bahr et al[8] reported that although none of their 27 sporadic BrS cases hosted an *SCN5A* mutation, 38% of their index cases with clearly familial BrS were positive. The number of sporadic versus familial BrS patients for each center's cohort is currently unknown. Alternatively, some of the lower yield centers may have accepted a greater proportion of weaker clinical cases for BrS genetic testing because no particular litmus test was demanded before acceptance of a sample.

Eight of the 9 centers represent research-based genetic testing laboratories, where most often the cohorts for such laboratories are composed of phenotypically robust cases of BrS. However, 1 center (center 5 in Table 1) represents a clinical laboratory offering the commercially available, fee-based genetic test for both BrS1 and LQTS. In this setting, the level of clinical suspicion and the usage of the genetic test by the referring physician are unknown for each patient sample submitted. Among their first 195 BrS referral cases submitted for clinical genetic testing, 22.6% were identified with a possible pathogenic *SCN5A* mutation, which is in line with the higher point estimate of a 20% prevalence of *SCN5A* mutations among clinically strong cases of BrS patients,[7] and consistent with the noncommercial centers in this compendium. In contrast, this laboratory has reported a yield of 36% for the first 2,500 consecutive unrelated LQTS referral cases tested compared with a yield of 75% among clinically strong cases of LQTS.[27] These observations suggest that in clinical practice, prescribing cardiologists are submitting higher-probability BrS cases for BrS1 genetic testing compared with LQTS.

In this compendium, 3% of the genotype-positive patients hosted multiple putative pathogenic *SCN5A* mutations, absent in control subjects. Akin to genotype–phenotype observations in LQTS,[28] patients hosting multiple *SCN5A* mutations were younger at diagnosis (29.7 ± 16 years) than those having a single mutation. Nearly half of the 13 cases (all male) with multiple mutations were younger than 25 years of age, with the youngest presenting at 2 years of age. Whether carriers of multiple mutations had a more severely expressed phenotype, such as having more multiple syncopal events, aborted cardiac arrest, or stronger family history of SCD, than single-mutation carriers is unknown.

Mutations in this compendium overwhelmingly represent "private" mutations, meaning they were seen only once. Nearly 80% of the 293 unique mutations were identified in a single unrelated case. Fewer than 20 mutations were seen in more than 3 unrelated BrS patients. However, nearly 10% of the 438 unrelated *SCN5A* mutation-positive patients hosted 1 of 4 mutations: E1784K (14 patients), F861WfsX90 (11 patients), D356N (8 patients), and G1408R (7 patients). In this compendium, more than one-third of the genotype-positive patients had radical or non-missense mutations (i.e., frameshift, nonsense, and splicing errors) that represent extremely high-probability case mutations (only 1 such variant was found in 1 of the 1,300 healthy volunteers) and would predictably cause a

Table 3 Brugada syndrome patients with multiple *SCN5A* mutations

Gender	Age at diagnosis (yrs)	Mutation 1	Location	Mutation 2	Location
M	35	N109K	N-terminal	V240M	DI-S4/S5
M	16	A185V	DI-S2/S3	A226V	DI-S4
M	44	611+1 G>A	DI-S3	V300I	DI-S5/S6
M	26	T220I	DI-S4	E439K	DI-DII
M	21	934+4 C>T	DI-S5/S6	G1642E	DIV-S4
M	51	P336L	DI-S5/S6	I1660V	DIV-S5
M	40	L619F	DI-DII	Q1383X	DII-S5/S6
M	49	T632M	DI-DII	M764R	DII-S2
M	2	Q646RfsX5	DI-DII	D1243N	DIII-S2
M	24	A647D	DI-DII	P1332L	DIII-S4/S5
M	7	G752R	DII-S2	K1872N	C-terminal
M	41	E1053K	DII-DIII	R1583C	DIV-S2/S3
M	23	R1232W	DIII-S1/S2	T1620M	DIV-S3/S4

M = male.

Table 4 Compendium of Brugada syndrome-associated *SCN5A* mutations

Region	Nucleotide change	Coding effect	Mutation type	Location	No. of unrelated individuals	Testing center
Exon 2	3 G>A	M1I*	Missense	N-terminal	1	1
Exon 2	53 G>A	R18Q*	Missense	N-terminal	1	3
Exon 2	191_193delTGC	L64del*	In-frame del	N-terminal	1	5
Exon 2	210 T>G	N70K*	Missense	N-terminal	1	5
Exon 2	217 C>T	Q73X*	Nonsense	N-terminal	1	2
Exon 2	250 G>A	D84N*	Missense	N-terminal	2	1
Exon 3	278 T>C	F93S*	Missense	N-terminal	1	1
Exon 3	281 T>G	I94S*	Missense	N-terminal	1	7
Exon 3	310 C>T	R104W*	Missense	N-terminal	2	1, 2
Exon 3	311 G>A	R104Q	Missense	N-terminal	3	1, 7, 8
Exon 3	327 C>A	N109K*	Missense	N-terminal	1	3
Exon 3	361 C>T	R121W*	Missense	N-terminal	1	8
Exon 3	362 G>A	R121Q*	Missense	N-terminal	2	2, 6
Exon 3	376 A>G	K126E	Missense	N-terminal	1	9
Exon 3	381dupT	L128SfsX44*	Frame shift	DI-S1	1	7
Intron 3	393 −5 C>A*		Splice site	DI-S1	1	1
Exon 4	407 T>C	L136P	Missense	DI-S1	2	8
Exon 4	410_418dupTCATGTGCA	I137_C139dup*	In-frame ins	DI-S1	1	3
Exon 4	436 G>A	V146M*	Missense	DI-S1	1	7
Exon 4	468 G>A	W156X	Nonsense	DI-S1/S2	1	3
Exon 4	477 T>A	Y159X*	Nonsense	DI-S2	1	5
Exon 4	481 G>C	E161Q*	Missense	DI-S2	1	6
Exon 4	481 G>A	E161K	Missense	DI-S2	3	3, 4
Exon 5	486delC	Y162XfsX1*	Frame shift	DI-S2	1	5
Exon 5	525 G>C	K175N*	Missense	DI-S2	1	1
Exon 5	533 C>G	A178G*	Missense	DI-S2	1	9
Exon 5	535 C>T	R179X	Nonsense	DI-S2/S3	1	2
Exon 5	544 T>C	C182R*	Missense	DI-S2/S3	1	4
Exon 5	554 C>T	A185V*	Missense	DI-S2/S3	1	2
Exon 5	579 G>A	W193X*	Nonsense	DI-S3	1	4
Exon 5	611 C>T	A204V*	Missense	DI-S3	1	4
Intron 5	611 +1 G>A*		Splice site	DI-S3	1	5
Intron 5	611 +3_611+4dupAA		Splice site	DI-S3	1	9
Intron 5	612 −2 A>G*		Splice site	DI-S3	1	4
Exon 6	635 T>A	L212Q*	Missense	DI-S3/S4	1	5
Exon 6	656_657insATTCA	T220FfsX10*	Frame shift	DI-S4	1	2
Exon 6	659 C>T	T220I	Missense	DI-S4	2	2, 3
Exon 6	664 C>T	R222X	Nonsense	DI-S4	4	2, 4
Exon 6	665 G>A	R222Q	Missense	DI-S4	1	4
Exon 6	667 G>C	V223L*	Missense	DI-S4	2	2
Exon 6	673 C>T	R225W	Missense	DI-S4	3	1, 6
Exon 6	677 C>T	A226V	Missense	DI-S4	2	2
Exon 6	694 G>A	V232I	Missense	DI-S4	2	2, 6
Exon 7	718 G>A	V240M	Missense	DI-S4/S5	1	3
Exon 7	745 A>T	K249X*	Nonsense	DI-S4/S5	1	6
Exon 7	808 C>A	Q270K*	Missense	DI-S5	1	6
Exon 7	827 T>A	L276Q	Missense	DI-S5	1	8
Exon 7	832 C>G	H278D*	Missense	DI-S5/S6	1	4
Exon 7	844 C>T	R282C*	Missense	DI-S5/S6	1	2
Exon 7	898 G>A	V300I*	Missense	DI-S5/S6	1	5
Intron 7	934 +1 G>A*		Splice site	DI-S5/S6	1	3
Intron 7	934 +4 C>T*		Splice site	DI-S5/S6	1	5
Exon 8	944 T>C	L315P*	Missense	DI-S5/S6	1	6
Exon 8	959 C>A	T320N*	Missense	DI-S5/S6	1	5
Exon 8	974 T>G	L325R	Missense	DI-S5/S6	1	4
Intron 8	998 +1 G>A*		Splice site	DI-S5/S6	1	4
Exon 9	1007 C>T	P336L	Missense	DI-S5/S6	2	2, 6
Exon 9	1036 G>T	E346X	Nonsense	DI-S5/S6	1	1
Exon 9	1052 G>T	G351V	Missense	DI-S5/S6	1	9
Exon 9	1052 G>A	G351D*	Missense	DI-S5/S6	1	2
Exon 9	1066 G>A	D356N	Missense	DI-S5/S6	8	1, 2, 4, 6, 7
Exon 9	1099 C>T	R367C	Missense	DI-S5/S6	2	3
Exon 9	1100 G>T	R367L*	Missense	DI-S5/S6	1	1

Table 4 Continued

Region	Nucleotide change	Coding effect	Mutation type	Location	No. of unrelated individuals	Testing center
Exon 9	1100 G>A	R367H	Missense	DI-S5/S6	6	1, 2, 8, 9
Exon 9	1106 T>A	M369K	Missense	DI-S5/S6	1	1
Exon 9	1120 T>G	W374G*	Missense	DI-S5/S6	1	1
Exon 9	1127 G>A	R376H	Missense	DI-S5/S6	4	3, 4, 8
Exon 10	1156 G>A	G386R*	Missense	DI-S5/S6	1	1
Exon 10	1157 G>A	G386E*	Missense	DI-S5/S6	2	2
Exon 10	1186 G>C	V396L*	Missense	DI-S6	1	1
Exon 10	1187 T>C	V396A*	Missense	DI-S6	1	2
Exon 10	1255 C>T	Q419X*	Nonsense	DI/DII	1	7
Exon 10	1315 G>A	E439K*	Missense	DI/DII	1	3
Intron 10	1338 +2 T>A*		Splice site	DI/DII	1	6
Exon 11	1428_1431delCAAG	S476RfsX30*	Frame shift	DI/DII	1	3
Exon 11	1502 A>G	D501G	Missense	DI/DII	1	3
Exon 12	1537delC	R513VfsX8*	Frame shift	DI/DII	1	8
Exon 12	1562delA	K521SfsX102*	Frame shift	DI/DII	1	2
Exon 12	1577 G>A	R526H*	Missense	DI/DII	2	1, 5
Exon 12	1595 T>G	F532C	Missense	DI/DII	1	2
Exon 12	1603 C>T	R535X	Nonsense	DI/DII	4	1, 2, 4, 5
Exon 12	1629 T>A	F543L*	Missense	DI/DII	1	2
Exon 12	1654 G>A	G552R*	Missense	DI/DII	1	9
Exon 12	1717 C>T	Q573X*	Nonsense	DI/DII	1	2
Exon 12	1721delG	G574DfsX49*	Frame shift	DI/DII	1	2
Exon 12	1844 G>A	G615E	Missense	DI/DII	1	4
Exon 12	1855 C>T	L619F	Missense	DI/DII	1	1
Exon 12	1858 C>T	R620C*	Missense	DI/DII	1	1
Exon 12	1890 G>A	T630T*	Silent/splice site	DI/DII	3	1, 3
Intron 12	1890 +5 G>A*		Splice site	DI/DII	2	2, 5
Exon 13	1895 C>T	T632M	Missense	DI/DII	2	2, 4
Exon 13	1918 C>G	P640A*	Missense	DI/DII	1	3
Exon 13	1936delC	Q646RfsX5*	Frame shift	DI/DII	3	2, 5, 6
Exon 13	1940 C>A	A647D*	Missense	DI/DII	1	5
Exon 13	1943 C>T	P648L	Missense	DI/DII	1	7
Exon 13	1950_1953delAGAT	D651AfsX25*	Frame shift	DI/DII	1	4
Exon 13	1981 C>T	R661W*	Missense	DI/DII	1	5
Exon 13	1983_1993dupGGCCCTCAGCG	A665GfsX16*	Frame shift	DI/DII	1	1
Exon 14	2024_2025delAG	E675VfsX45*	Frame shift/splice	DI/DII	1	2
Exon 14	2047 T>G	C683G*	Missense	DI/DII	1	7
Exon 14	2092 G>T	E698X*	Nonsense	DI/DII	1	2
Exon 14	2102 C>T	P701L	Missense	DI/DII	1	4
Exon 14	2150 C>T	P717L*	Missense	DII-S1	1	6
Exon 14	2201dupT	M734IfsX11*	Frame shift	DII-S1	1	7
Exon 14	2204 C>T	A735V	Missense	DII-S1	4	2, 4, 8, 9
Exon 14	2236 G>A	E746K	Missense	DII-S1/S2	3	1, 2, 7
Exon 14	2254 G>A	G752R	Missense	DII-S2	5	1, 5
Exon 15	2273 G>A	G758E*	Missense	DII-S2	1	2
Exon 15	2274delG	I759FfsX6*	Frame shift	DII-S2	2	5
Exon 15	2291 T>G	M764R*	Missense	DII-S2	1	4
Exon 15	2314 G>A	D772N	Missense	DII-S2/S3	1	1
Exon 15	2317 C>T	P773S*	Missense	DII-S2/S3	1	6
Exon 15	2320delT	Y774TfsX28*	Frame shift	DII-S2/S3	2	3
Exon 15	2326_2328delTAC	Y776del*	In-frame del	DII-S2/S3	1	2
Exon 15	2365 G>A	V789I*	Missense	DII-S3	1	4
Exon 15	2423 G>C	R808P*	Missense	DII-S4	1	1
Exon 15	2435_2436+3delTGGTAinsCGCCT	L812P†*	Indel/splice site	DII-S4	1	5
Exon 16	2465 G>A	W822X	Nonsense	DII-S4	1	4
Exon 16	2516 T>C	L839P*	Missense	DII-S4/S5	1	1
Exon 16	2533delG	V845CfsX2*	Frame shift	DII-S5	1	6
Exon 16	2549_2550insTG	F851GfsX19*	Frame shift	DII-S5	1	2
Exon 16	2550_2551dupGT	F851CfsX19*	Frame shift	DII-S5	1	5
Exon 16	2553 C>A	F851L	Missense	DII-S5	1	2
Exon 16	2582_2583delTT	F861WfsX90	Frame shift	DII-S5	11	3, 7
Exon 16	2599 G>C	E867Q*	Missense	DII-S5/S6	1	2
Exon 16	2602delC	L868X	Frame shift	DII-S5/S6	2	6, 7

Table 4 Continued

Region	Nucleotide change	Coding effect	Mutation type	Location	No. of unrelated individuals	Testing center
Exon 16	2632 C>T	R878C	Missense	DII-S5/S6	1	2
Exon 16	2633 G>A	R878H*	Missense	DII-S5/S6	5	1, 2, 4, 5, 7
Exon 16	2657 A>C	H886P*	Missense	DII-S5/S6	1	2
Exon 16	2677 C>T	R893C*	Missense	DII-S5/S6	2	4
Exon 16	2678 G>A	R893H*	Missense	DII-S5/S6	3	1, 3, 4
Exon 16	2701 G>A	E901K*	Missense	DII-S5/S6	3	1, 4
Exon 16	2729 C>T	S910L	Missense	DII-S5/S6	1	1
Exon 16	2743 T>C	C915R*	Missense	DII-S6	1	3
Exon 16	2750 T>G	L917R*	Missense	DII-S6	1	2
Exon 16	2780 A>G	N927S	Missense	DII-S6	3	3, 7
Exon 16	2783 T>C	L928P*	Missense	DII-S6	1	1
Exon 17	2804 T>C	L935P*	Missense	DII-S6	1	5
Exon 17	2850delT	D951MfsX6*	Frame shift	DII/DIII	1	4
Exon 17	2893 C>T	R965C	Missense	DII/DIII	3	2, 4, 5
Exon 17	2894 G>A	R965H	Missense	DII/DIII	1	3
Exon 17	2914_2923delTTTGTCAAGC	F972GfsX170*	Frame shift	DII/DIII	1	6
Exon 17	2989 G>A	A997T*	Missense	DII/DIII	1	5
Exon 17	3005_3012delCCAGCTGC	P1002HfsX25*	Frame shift	DII/DIII	1	7
Exon 17	3140_3141dupTG	P1048CfsX98*	Frame shift	DII/DIII	1	3
Exon 17	3157 G>A	E1053K	Missense	DII/DIII	3	1
Exon 17	3164 A>G	D1055G*	Missense	DII/DIII	1	1
Exon 17	3171_3172delTGinsA	D1057EfsX88*	Insertion/deletion	DII/DIII	1	7
Intron 17	3228 +2delT*		Splice site	DII/DIII	1	3
Exon 18	3236 C>A	S1079Y*	Missense	DII/DIII	1	1
Exon 18	3338 C>T	A1113V*	Missense	DII/DIII	1	5
Exon 18	3345 G>A	W1115X*	Nonsense	DII/DIII	1	6
Exon 19	3419 G>C	S1140T*	Missense	DII/DIII	1	5
Exon 20	3553_3554delCA	Q1185GfsX55*	Frame shift	DII/DIII	1	3
Exon 20	3576 G>A	W1192X*	Nonsense	DII/DIII	1	6
Exon 20	3622 G>T	E1208X	Nonsense	DIII-S1	1	1
Exon 20	3634_3636delATC	I1212del*	In-frame del	DIII-S1	1	2
Exon 20	3656 G>A	S1219N	Missense	DIII-S1	1	1
Exon 20	3666delG	A1223PfsX7*	Frame shift/splice	DIII-S1	1	1
Exon 21	3673 G>A	E1225K	Missense	DIII-S1/S2	4	1, 5, 6, 7
Exon 21	3682 T>C	Y1228H	Missense	DIII-S1/S2	1	1
Exon 21	3694 C>T	R1232W	Missense	DIII-S1/S2	3	1, 2, 9
Exon 21	3695 G>A	R1232Q*	Missense	DIII-S1/S2	1	7
Exon 21	3716 T>C	L1239P*	Missense	DIII-S2	1	2
Exon 21	3727 G>A	D1243N*	Missense	DIII-S2	5	1, 2, 5
Exon 21	3746 T>A	V1249D*	Missense	DIII-S2	1	6
Exon 21	3758 A>G	E1253G*	Missense	DIII-S2	1	1
Exon 21	3784 G>A	G1262S	Missense	DIII-S2	1	1
Exon 21	3813 G>C	W1271C*	Missense	DIII-S3	1	1
Exon 21	3823 G>A	D1275N	Missense	DIII-S3	3	1, 5
Intron 21	3840 +1 G>A		Splice site	DIII-S3	6	1, 3, 4
Exon 22	3863 C>G	A1288G*	Missense	DIII-S3	1	4
Exon 22	3894delC	I1299SfsX13*	Frame shift	DIII-S4	1	5
Exon 22	3932 T>C	L1311P*	Missense	DIII-S4	1	7
Exon 22	3956 G>T	G1319V	Missense	DIII-S4/S5	5	2, 3, 7
Intron 22	3963 +4 A>G*		Splice site	DIII-S4/S5	1	5
Intron 22	3963 +2 T>C		Splice site	DIII-S4/S5	1	1
Exon 23	3968 T>G	V1323G*	Missense	DIII-S4/S5	1	7
Exon 23	3995 C>T	P1332L	Missense	DIII-S4/S5	1	5
Exon 23	4018 G>A	V1340I*	Missense	DIII-S5	1	9
Exon 23	4030 T>C	F1344L*	Missense	DIII-S5	1	1
Exon 23	4036 C>A	L1346I*	Missense	DIII-S5	1	4
Exon 23	4037 T>C	L1346P*	Missense	DIII-S5	1	3
Exon 23	4052 T>G	M1351R*	Missense	DIII-S5	1	2
Exon 23	4057 G>A	V1353M*	Missense	DIII-S5	2	2
Exon 23	4072 G>T	G1358W*	Missense	DIII-S5	1	4
Exon 23	4077 G>T	K1359N*	Missense	DIII-S5	1	4
Exon 23	4079 T>G	F1360C	Missense	DIII-S5/S6	1	1
Exon 23	4088 G>A	C1363Y	Missense	DIII-S5/S6	1	3

Table 4 Continued

Region	Nucleotide change	Coding effect	Mutation type	Location	No. of unrelated individuals	Testing center
Exon 23	4118 T>A	L1373X*	Nonsense	DIII-S5/S6	1	2
Exon 23	4145 G>T	S1382I	Missense	DIII-S5/S6	1	1
Exon 23	4147 C>T	Q1383X*	Nonsense	DIII-S5/S6	1	1
Exon 23	4178 T>A	L1393X	Nonsense	DIII-S5/S6	3	1, 3, 9
Exon 23	4182 C>G	Y1394X*	Nonsense	DIII-S5/S6	1	5
Exon 23	4190delA	K1397RfsX2	Frame shift	DIII-S5/S6	1	9
Exon 23	4213 G>A	V1405M*	Missense	DIII-S5/S6	2	1, 7
Exon 23	4213 G>C	V1405L	Missense	DIII-S5/S6	2	3
Exon 23	4216 G>C	G1406R	Missense	DIII-S5/S6	1	3
Exon 23	4217 G>A	G1406E*	Missense	DIII-S5/S6	2	5
Exon 23	4222 G>A	G1408R	Missense	DIII-S5/S6	7	1, 4, 5, 7
Exon 23	4226 A>G	Y1409C*	Missense	DIII-S5/S6	1	1
Exon 23	4227 C>G	Y1409X*	Nonsense	DIII-S5/S6	1	8
Exon 23	4234 C>T	L1412F*	Missense	DIII-S5/S6	1	5
Exon 24	4255 A>G	K1419E*	Missense	DIII-S5/S6	1	1
Exon 24	4258 G>C	G1420R*	Missense	DIII-S5/S6	1	3
Exon 24	4279 G>T	A1427S*	Missense	DIII-S5/S6	1	2
Exon 24	4283 C>T	A1428V*	Missense	DIII-S5/S6	1	2
Exon 24	4294 A>G	R1432G	Missense	DIII-S5/S6	1	4
Exon 24	4296 G>C	R1432S*	Missense	DIII-S5/S6	1	2
Exon 24	4298 G>T	G1433V*	Missense	DIII-S5/S6	1	3
Exon 24	4299 G>A	G1433G*	Silent/splice site	DIII-S5/S6	1	4
Intron 24	4299 +1 G>T*		Splice site	DIII-S5/S6	1	5
Intron 24	4299 +1delG*		Splice site	DIII-S5/S6	1	1
Intron 24	4300 −1 G>A*		Splice site	DIII-S5/S6	1	2
Exon 25	4302 T>G	Y1434X*	Nonsense	DIII-S5/S6	1	5
Exon 25	4313 C>T	P1438L	Missense	DIII-S5/S6	1	4
Exon 25	4320 G>A	W1440X	Nonsense	DIII-S5/S6	1	2
Exon 25	4321 G>C	E1441Q*	Missense	DIII-S5/S6	1	7
Exon 25	4342 A>C	I1448L*	Missense	DIII-S6	1	4
Exon 25	4343 T>C	I1448T*	Missense	DIII-S6	1	2
Exon 25	4346 A>G	Y1449C*	Missense	DIII-S6	1	1
Exon 25	4352 T>A	V1451D*	Missense	DIII-S6	1	5
Exon 25	4376_4379delTCTT	F1459SfsX3*	Frame shift	DIII-S6	1	6
Exon 25	4387 A>T	N1463Y*	Missense	DIII-S6	1	2
Exon 25	4389_4396delCCTCTTTA	L1464WfsX5*	Frame shift	DIII-S6	1	8
Exon 25	4402 G>T	V1468F*	Missense	DIII-S6	1	2
Exon 25	4426 C>T	Q1476X*	Nonsense	DIII/DIV	1	4
Intron 25	4437 +5 G>A*		Splice site	DIII/DIV	2	3, 5
Exon 26	4477_4479delAAG	K1493del*	In-frame del	DIII/DIV	2	1, 7
Exon 26	4477 A>T	K1493X*	Nonsense	DIII/DIV	1	2
Exon 26	4501 C>G	L1501V	Missense	DIII/DIV	1	1
Exon 27	4562 T>A	I1521K*	Missense	DIII/DIV	1	5
Exon 27	4573 G>A	V1525M*	Missense	DIV-S1	1	4
Exon 27	4642 G>A	E1548K*	Missense	DIV-S1/S2	3	1, 4
Exon 27	4708_4710dupATC	I1570dup*	In-frame ins	DIV-S2	1	3
Exon 27	4712 T>G	F1571C*	Missense	DIV-S2	1	4
Exon 27	4720 G>A	E1574K	Missense	DIV-S2	4	2, 6, 7
Exon 27	4745 T>C	L1582P*	Missense	DIV-S2	1	3
Exon 27	4747 C>T	R1583C*	Missense	DIV-S2/S3	2	1, 2
Exon 27	4748 G>A	R1583H*	Missense	DIV-S2/S3	1	1
Exon 27	4773 G>A	W1591X*	Nonsense	DIV-S3	1	2
Exon 27	4810 G>A	V1604M*	Missense	DIV-S3	1	1
Exon 27	4813 +2_4813+5dupTGGG		Splice site	DIV-S3	1	2
Exon 28	4838 A>T	Q1613L*	Missense	DIV-S3/S4	1	1
Exon 28	4845 C>A	Y1615X*	Nonsense	DIV-S3/S4	1	2
Exon 28	4856delC	P1619RfsX12*	Frame shift	DIV-S3/S4	1	2
Exon 28	4859 C>T	T1620M	Missense	DIV-S3/S4	2	2, 9
Exon 28	4867 C>T	R1623X	Nonsense	DIV-S4	2	2, 3
Exon 28	4868 G>A	R1623Q	Missense	DIV-S4	1	5
Exon 28	4885 C>T	R1629X*	nonsense	DIV-S4	1	3
Exon 28	4886 G>A	R1629Q*	Missense	DIV-S4	1	3
Exon 28	4912 C>T	R1638X	Nonsense	DIV-S4	3	2, 3

Table 4 Continued

Region	Nucleotide change	Coding effect	Mutation type	Location	No. of unrelated individuals	Testing center
Exon 28	4925 G>A	G1642E*	Missense	DIV-S4	1	5
Exon 28	4978 A>G	I1660V	Missense	DIV-S5	5	2, 3, 5, 6
Exon 28	4981 G>A	G1661R*	Missense	DIV-S5	2	1
Exon 28	4981 G>C	G1661R*	Missense	DIV-S5	1	2
Exon 28	4999 G>A	V1667I	Missense	DIV-S5	1	3
Exon 28	5015 C>A	S1672Y	Missense	DIV-S5	2	1, 4
Exon 28	5038 G>A	A1680T	Missense	DIV-S5	2	2, 6
Exon 28	5068_5070delGA	D1690HfsX98*	Frame shift	DIV-S5/S6	1	1
Exon 28	5083 C>T	Q1695X	Nonsense	DIV-S5/S6	2	1, 4
Exon 28	5092 G>A	A1698T*	Missense	DIV-S5/S6	1	2
Exon 28	5124_5126delCAC	T1709del*	In-frame del	DIV-S5/S6	1	4
Exon 28	5126 C>T	T1709M	Missense	DIV-S5/S6	2	1, 8
Exon 28	5126 C>G	T1709R*	Missense	DIV-S5/S6	1	4
Exon 28	5134 G>A	G1712S*	Missense	DIV-S5/S6	1	7
Exon 28	5141 A>G	D1714G	Missense	DIV-S5/S6	1	3
Exon 28	5157delC	I1720SfsX67*	Frame shift	DIV-S5/S6	1	8
Exon 28	5164 A>G	N1722D*	Missense	DIV-S5/S6	1	1
Exon 28	5182 T>C	C1728R*	Missense	DIV-S5/S6	1	2
Exon 28	5184 C>G	C1728W*	Missense	DIV-S5/S6	1	2
Exon 28	5218 G>A	G1740R	Missense	DIV-S5/S6	1	3
Exon 28	5227 G>A	G1743R	Missense	DIV-S5/S6	5	4, 5, 7, 9
Exon 28	5228 G>A	G1743E	Missense	DIV-S5/S6	6	2, 3
Exon 28	5290delG	V1764SfsX23*	Frame shift	DIV-S6	1	8
Exon 28	5290 G>T	V1764F	Missense	DIV-S6	1	7
Exon 28	5336 C>T	T1779M	Missense	C-terminal	1	2
Exon 28	5350 G>A	E1784K	Missense	C-terminal	14	1, 2, 5, 6, 7
Exon 28	5356_5357delCT	L1786EfsX2*	Frame shift	C-terminal	2	1
Exon 28	5387_5388insTGA	1795_1796insD	In-frame ins	C-terminal	1	3
Exon 28	5420dupA	F1808IfsX3*	Frame shift	C-terminal	1	7
Exon 28	5435 C>A	S1812X	Nonsense	C-terminal	1	7
Exon 28	5464_5467delTCTG	E1823HfsX10*	Frame shift	C-terminal	1	2
Exon 28	5494 C>G	Q1832E*	Missense	C-terminal	1	6
Exon 28	5577_5578dupAA	R1860KfsX13*	Frame shift	C-terminal	1	2
Exon 28	5581 G>A	V1861I*	Missense	C-terminal	1	2
Exon 28	5616 G>C	K1872N*	Missense	C-terminal	1	5
Exon 28	5707 G>C	S1904L	Missense	C-terminal	1	2
Exon 28	5770 G>A	A1924T	Missense	C-terminal	1	3
Exon 28	5803 G>A	G1935S	Missense	C-terminal	1	2
Exon 28	5812 G>A	E1938K*	Missense	C-terminal	1	2
Exon 28	6010_6012dupTTC	F2004dup*	In-frame ins	C-terminal	1	7
Exon 28	6010 T>G	F2004V*	Missense	C-terminal	1	5

del = deletion; dup = duplication; ins = insertion; indel = insertion/deletion; ins = insertion; * = novel mutation; Testing Center: 1 = Nantes; 2 = Brugada; 3 = AMC; 4 = Paris; 5 = PGxHealth; 6 = MMRL; 7 = UKM; 8 = NCVC; 9 = BCM.

significant loss of sodium channel function through a mechanism of haploinsufficiency. Recently, Meregalli et al[29] reported that BrS patients with truncation mutations, caused by radical mutations, had a more severe phenotype characterized as a higher propensity for syncope and prevalence of SCD among young first-degree relatives, than those BrS patients hosting missense mutations functionally characterized with ≤90% peak sodium current reduction.

The *SCN5A*-encoded cardiac voltage-gated sodium channel (Nav1.5), which is responsible for the initial fast upstroke of the cardiac action potential and accordingly plays a vital role in the excitability of myocardial cells and the proper conduction of the electrical pulsation of the heart, consists of 4 homologous domains (DI-DIV) that are connected by intracellular linkers. Each domain contains 6 transmembrane-spanning segments (S1-S6). Although case mutations were scattered throughout Nav1.5, there was clustering of putative BrS1-associated mutations whereby nearly three-fourths localized to the transmembrane and pore-forming domains compared with <20% of the rare variants found among the control subjects. Further, nearly 10% of patients with clinically suspected BrS had a mutation localizing to the channel's pore/selectivity filter (segments S5 and S6 and the interconnecting P-loops) compared with <0.5% of the control subjects. Because of the extreme rarity of pore-localizing missense variants among the healthy control subjects, such missense mutations found in cases are high probability BrS1-causative mutations. However, whether BrS1 patients with pore mutations behaved more poorly than those with mutations localizing to other domains was unable to be gleaned in this study.

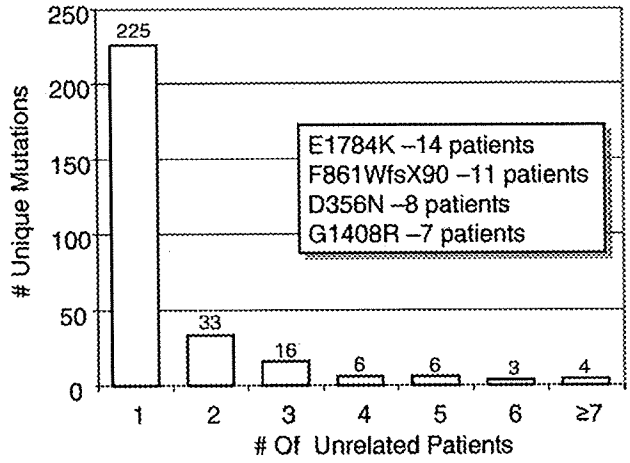

Figure 2 BrS1-associated mutation frequency distribution. This bar graph summarizes the distribution of specific mutations among unrelated patients. The Y-axis depicts the number of unique BrS1-associated mutations, and the X-axis represents the number of unrelated patients. For example, the first column indicates that there were 226 unique mutations each observed only once. The last column indicates that 4 different BrS1-associated mutations were each seen in ≥7 unrelated patients. The inset shows the 4 most common BrS1-associated mutations identified and the number of specified unrelated patients in whom the mutations were found.

In contrast, only 25 patients hosted a single missense mutation residing in either the DI-DII or DII-DIII linker domains. The observed preponderance (over 50% of which localize to these 2 IDLs) of the 42 unique rare missense variants identified in the healthy control subjects suggest that some of the 21 IDL localizing, possible BrS1-associated missense mutations that were identified in 25 cases may in fact represent false positives.[11,13] Despite being absent in over 1,300 control subjects, either cosegregation or functional studies on these DI-DII and DII-DIII linker-localizing mutations should be considered before upgrading their status from a rare variant of uncertain significance to a probable BrS1-causative missense mutation. For example, 1 of the 21 missense mutations, G615E, has been previously characterized as having no significant changes in current density or kinetics compared with wild type, casting some doubt on its level of causality.[25]

Whereas loss-of-function mutations in SCN5A have been shown to serve as a pathogenic basis for BrS, gain-of-function mutations in SCN5A provide the pathogenic substrate for LQT3, a clinically and mechanistically distinct arrhythmia syndrome from BrS. Interestingly, 10 mutations identified in this BrS compendium have been implicated previously in LQTS, including the most commonly observed mutation, E1784K. In fact, E1784K represented the most commonly observed SCN5A mutation (4/26, ~15%) among a cohort of 541 unrelated LQTS patients.[28] Although the clinical phenotype for the patients hosting 1 of these 10 mutations could have been assigned incorrectly, it is far more likely that these represent overlap syndrome/mixed phenotype syndrome–associated *SCN5A* mutations.

For example, E1784K represents the quintessential example of a cardiac sodium channel mutation with the capacity to provide for a mixed clinical phenotype of LQT3, BrS, and conduction disorders.[30] Makita et al[30] reported recently a high prevalence of LQT3/BrS/conduction phenotype overlap among 41 E1784K carriers from 15 kindreds of diverse ethnic background. Of the 41 cases, 93% displayed a prolonged QTc, 22% with a diagnostic indicator (ST-segment elevation or positive provocation test) of BrS, and 39% had sinus node dysfunction. Functional characterization of mutant E1784K sodium channels displayed unique biophysical and pharmacological properties consistent with other mutations that yield a mixed phenotype, including a negative shift of steady-state sodium channel activation and enhanced tonic block in response to sodium channel blockers, leading to an additional BrS/sinus node dysfunction phenotype in conjunction with a prolonged QTc.[30] This particular functional effect may influence the pharmacological management of patients with E1784K-SCN5A disease.[30]

Similarly, Bezzina et al[31] in 1999, described an LQT3/BrS overlap phenotype in a large 1795insD-SCN5A mutation–positive 8-generation kindred characterized with a high incidence of sudden nocturnal death, QT-interval prolongation, and Brugada ECG. Whether or not the 9 other mutations, identified here in BrS patients and elsewhere in patients purported to have LQTS, have a similar functional characteristic that provides a substrate for producing a mixed/overlapping clinical phenotype remains to be seen.

Given that *SCN5A* remains the most common BrS genotype despite accounting for only 20% of BrS, genetic heterogeneity of the disease is evident and the role of genetic background in the pathophysiology of BrS is important.[32] Recently, mutations in the glycerol-3-phosphate dehydrogenase 1–like protein encoded by *GPD1L* have been shown to affect trafficking of the sodium channel to the plasma membrane, thus reducing overall sodium current, giving rise to the BrS phenotype.[33] Recently, mutations involving the L-type calcium channel alpha and beta subunits encoded by the *CACNA1C* and *CACNB2b* genes,

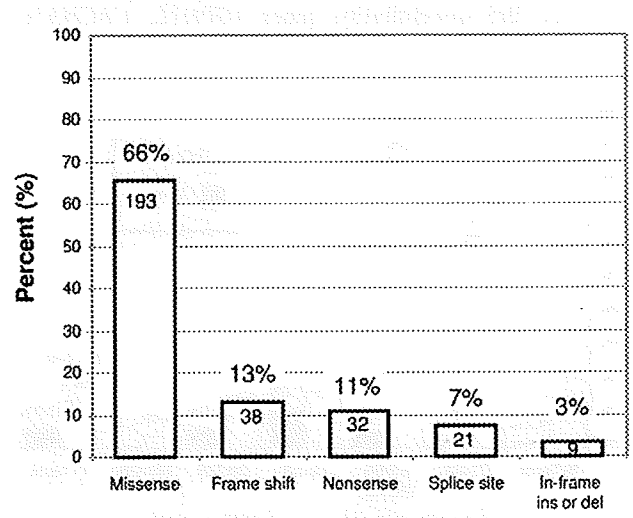

Figure 3 Summary of *SCN5A* mutation type for BrS1. The distribution of mutation type (missense, frameshift, etc.) is summarized for the possible BrS1-associated *SCN5A* mutations. The number within the column represents the total number of unique mutations for the respective type. For example, there were 193 unique missense mutations identified.

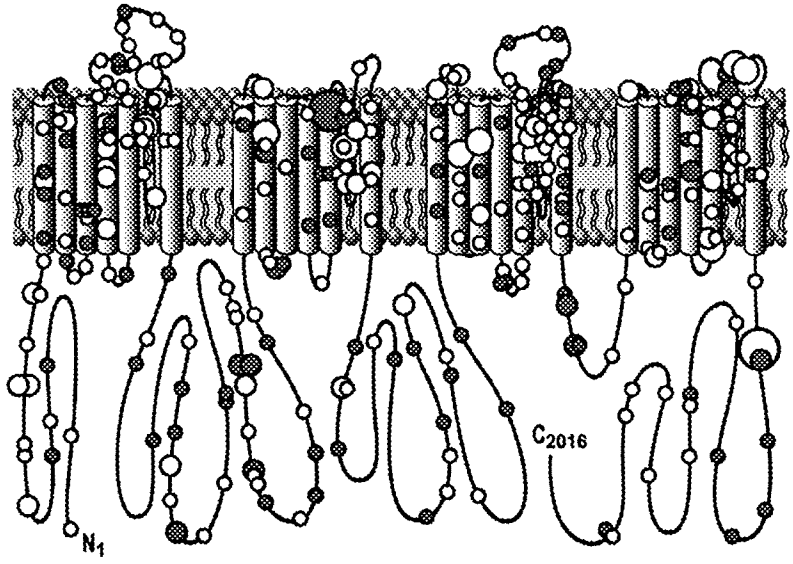

Figure 4 Channel topology of NaV1.5's pore-forming alpha subunit encoded by *SCN5A* and location of putative BrS1-causing mutations. Missense mutations are indicated by white circles, whereas mutations other than missense (i.e., frameshift, deletions, splice-site, etc.) are depicted as gray circles. In addition, 4 different circle sizes are used, with the smallest circle indicating a mutation seen only once; a medium-sized circle for mutations observed in 2, 3, or 4 unrelated patients; a large circle for mutations observed in 5, 6, 7, 8, or 9 patients; and the largest circle indicating those mutations observed in at least 10 unrelated patients.

respectively, were implicated in nearly 11% of BrS cases.[34] Other minor causes of BrS include mutations in the sodium channel beta 1 subunit encoded by *SCN1B* and in a putative beta subunit of the transient outward potassium channel (I_{to}) encoded by *KCNE3*.[35,36] The most recent gene associated with BrS is the *SCN3B*-encoded beta-3 subunit of the cardiac sodium channel.[37]

A number of these minor BrS-susceptibility genes function in part as sodium channel interacting proteins (ChIPs). The cardiac sodium channel is now understood to be a part of a macromolecular complex, with numerous ChIPs regulating its expression, localization, and function. As exemplified by *GPD1L*, *SCN1B*, and *SCN3B*, other genes, which encode other sodium ChIPs whose disruption would portend a loss of function sodium channel phenotype, would warrant examination as candidate BrS disease or disease-modifying genes. These 6 minor BrS-susceptibility genes (*GPD1L*, *CACNA1C*, *CACNB2B*, *SCN1B*, *SCN3B*, and *KCNE3*) have not been examined among the remaining 1,673 *SCN5A*-negative unrelated cases represented in this compendium, but it is predicted that these minor genes will explain <10% of this cohort. Thus, the majority of BrS still remains genetically elusive.

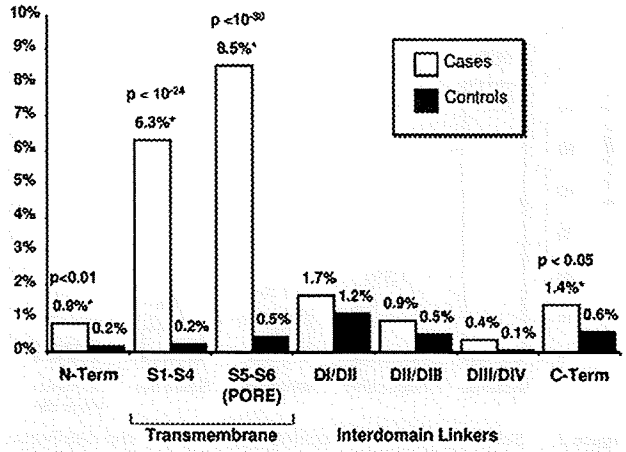

Figure 5 Yield of missense mutations/rare variants in cases and control subjects by location. A comparison of the yield of rare, missense case mutations/control variants in 2,111 cases versus 1,300 control subjects by protein location. * = $p<0.05$.

Study limitations

For the purpose of this compendium of identified mutations, only minimal demographic information from each center's cohort was made available because the focus was on the prevalence, spectrum, and localization of *SCN5A* mutations among suspected cases of BrS rather than an attempt to establish any particular genotype–phenotype correlates. Nevertheless, there is significant clinical value due to the data in aggregate. For example, the rare missense mutations seen numerous times among these cases referred for BrS genetic testing, and still not among the control subjects, indicate high-probability BrS-associated mutations.

Furthermore, despite the lack of clinical information, the physical distribution of mutations/variants among cases and control subjects is very telling, whereby the power in numbers can come from the series of mutations/variants clustering in a region, even if the individual mutations/variants have only been observed rarely. For example, even without cosegregation data or in vitro function analyses, the next rare, nonmissense mutation as well as the next transmembrane-localizing missense mutation represent high-probability pathogenic substrates. Conversely, those rare single amino acid substitutions localizing to the domain I-II and II-III linkers should be buttressed with either clinical cosegregation data or in vitro functional data before being upgraded from this list of possible deleterious mutations to highly probable deleterious mutations.

Additionally, this analysis focused on only identifying coding and splicing region single-nucleotide mutations and small insertion/deletion mutations by molecular techniques that often do not detect larger rearrangements, insertions, and deletions.

SCN5A promoter region mutations, deep intronic mutations, epigenetic methylation mutations, and large genomic rearrangements, all of which could predictably produce a loss-of-function phenotype, would have escaped detection by the mutational analyses performed herein. However, such alterations are quite uncommon when compared with changes in the known coding sequences of the genes.

Despite these limitations, this compendium of nearly 300 distinct BrS-associated mutations provides key observations that may assist in the further interrogation of the cardiac sodium channel biology and serve as a foundation for the development of algorithms to assist in distinguishing pathogenic mutations from similarly rare but otherwise innocuous ones.

Conclusion

Since the sentinel discovery of BrS as a cardiac channelopathy in 1998, our genomic understanding of this potentially lethal disorder has matured from a phase of discovery to one of translational medicine. This international consortium of BrS genetic testing centers has tripled the catalog of possible BrS1-associated mutations with the addition of 200 new mutations to the public domain and has provided a template to draw upon for further genetic testing interpretation and biological inquiry.

References

1. Chen PS, Priori SG. The Brugada syndrome. J Am Coll Cardiol 2008;51:1176–1180.
2. Meregalli PG, Wilde AAM, Tan HL. Pathophysiological mechanisms of Brugada syndrome: depolarization disorder, repolarization disorder, or more? Cardiovasc Res 2005;67:367–378.
3. Antzelevitch C, Brugada P, Borggrefe M, et al. Brugada syndrome: report of the second consensus conference. Heart Rhythm 2005;2:429–440. Erratum: Heart Rhythm 2005;2:905.
4. Tester DJ, Ackerman MJ. Cardiomyopathic and channelopathic causes of sudden unexplained death in infants and children. Annu Rev Med 2009;60:69–84.
5. Brugada P, Brugada J. Right bundle branch block, persistent ST segment elevation and sudden cardiac death: a distinct clinical and electrocardiographic syndrome. A multicenter report. J Am Coll Cardiol 1992;20:1391–1396.
6. Priori SG, Napolitano C, Gasparini M, et al. Clinical and genetic heterogeneity of right bundle branch block and ST-segment elevation syndrome: a prospective evaluation of 52 families. Circulation 2000;102:2509–2515.
7. Priori SG, Napolitano C, Gasparini M, et al. Natural history of Brugada syndrome: insights for risk stratification and management. Circulation 2002;105:1342–1347.
8. Schulze-Bahr E, Eckardt L, Breithardt G, et al. Sodium channel gene (SCN5A) mutations in 44 index patients with Brugada syndrome: different incidences in familial and sporadic disease. Hum Mutat 2003;21:651–652. Erratum: Hum Mutat 2005;26:61.
9. Remme CA, Wilde AAM. SCN5A overlap syndromes: no end to disease complexity? [Comment.] Europace 2008;10:1253–255.
10. Zimmer T, Surber R. SCN5A channelopathies—an update on mutations and mechanisms. Prog Biophys Mol Biol 2008:98(2–3):120–136.
11. Ackerman MJ, Splawski I, Makielski JC, et al. Spectrum and prevalence of cardiac sodium channel variants among black, white, Asian, and Hispanic individuals: implications for arrhythmogenic susceptibility and Brugada/long QT syndrome genetic testing [see Comment]. Heart Rhythm 2004;1:600–607.
12. Spiegelman JI, Mindrinos MN, Oefner PJ. High-accuracy DNA sequence variation screening by DHPLC. BioTechniques 2000;29:1084–1092.
13. Kapa S, Tester DJ, Salisbury BA, et al. Genetic testing for long QT syndrome—distinguishing pathogenic mutations from benign variants. Circulation 2009;120(18):1752–1760.
14. den Dunnen JT, Antonarakis SE. Nomenclature for the description of human sequence variations. Hum Genet 2001;109:121–124.
15. Murray A, Donger C, Fenske C, et al. Splicing mutations in KCNQ1: a mutation hot spot at codon 344 that produces in frame transcripts. Circulation 1999;100:1077–1084.
16. Zhuang Y, Weiner AM. A compensatory base change in U1 snRNA suppresses a 5′ splice site mutation. Cell 1986;46:827–835.
17. Rogan PK, Svojanovsky S, Leeder JS. Information theory-based analysis of CYP2C19, CYP2D6 and CYP3A5 splicing mutations. Pharmacogenetics 2003;13:207–218.
18. Splawski I, Shen J, Timothy K, Vincent GM, Lehmann MH, Keating MT. Genomic structure of three long QT syndrome genes: KVLQT1, HERG, and KCNE1. Genomics 1998;51:86–97.
19. Wang Q, Li Z, Shen J, Keating MT. Genomic organization of the human SCN5A gene encoding the cardiac sodium channel. Genomics 1996;34:9–16.
20. Neyroud N, Richard P, Vignier N, et al. Genomic organization of the KCNQ1 K+ channel gene and identification of C-terminal mutations in the long-QT syndrome. Circ Res 1999;84:290–297.
21. Wehrens XHT, Rossenbacker T, Jongbloed RJ, et al. A novel mutation L619F in the cardiac Na+ channel SCN5A associated with long-QT syndrome (LQT3): a role for the I-II linker in inactivation gating. Hum Mutat 2003;21:552.
22. Ruan Y, Liu N, Bloise R, Napolitano C, Priori SG. Gating properties of SCN5A mutations and the response to mexiletine in long-QT syndrome type 3 patients. Circulation 2007;116:1137–1144.
23. Kambouris NG, Nuss HB, Johns DC, Tomaselli GF, Marban E, Balser JR. Phenotypic characterization of a novel long-QT syndrome mutation (R1623Q) in the cardiac sodium channel. Circulation 1998;97:640–644.
24. Wei J, Wang DW, Alings M, et al. Congenital long-QT syndrome caused by a novel mutation in a conserved acidic domain of the cardiac Na+ channel. Circulation 1999;99:3165–3171.
25. Yang P, Kanki H, Drolet B, et al. Allelic variants in long-QT disease genes in patients with drug-associated torsades de pointes. Circulation 2002;105:1943–1948.
26. Chen Q, Kirsch GE, Zhang D, et al. Genetic basis and molecular mechanism for idiopathic ventricular fibrillation. Nature 1998;392:293–296.
27. Kapplinger JD, Tester DJ, Salisbury BA, et al. Spectrum and prevalence of mutations from the first 2500 consecutive unrelated patients referred for the *FAMILION*® long QT syndrome genetic test. Heart Rhythm 2009:6:1297–1303.
28. Tester DJ, Will ML, Haglund CM, Ackerman MJ. Compendium of cardiac channel mutations in 541 consecutive unrelated patients referred for long QT syndrome genetic testing. Heart Rhythm 2005;2:507–517.
29. Meregalli PG, Tan HL, Probst V, et al. Type of SCN5A mutation determines clinical severity and degree of conduction slowing in loss-of-function sodium channelopathies. Heart Rhythm 2009;6:341–348.
30. Makita N, Behr E, Shimizu W, et al. The E1784K mutation in SCN5A is associated with mixed clinical phenotype of type 3 long QT syndrome. J Clin Invest 2008;118:2219–2229.
31. Bezzina C, Veldkamp MW, van den Berg MP, et al. A single Na^+ channel mutation causing both long-QT and brugada syndromes. Circ Res 1999;85:1206–1213.
32. Probst V, Wilde AAM, Barc J, et al. *SCN5A* Mutations and the role of genetic background in the pathophysiology of brugada syndrome. Circ Cardiovasc Genet 2009; accepted manuscript, in press.
33. London B, Michalec M, Mehdi H, et al. Mutation in glycerol-3-phosphate dehydrogenase 1 like gene (GPD1-L) decreases cardiac Na+ current and causes inherited arrhythmias. Circulation 2007;116:2260–2268.
34. Antzelevitch C. Genetic basis of Brugada syndrome [Comment]. Heart Rhythm 2007;4:756–757. Erratum: Heart Rhythm 2007;4:990.
35. Watanabe H, Koopman TT, Scouarnec SL, et al. Sodium channel β1 subunit mutations associated with Brugada syndrome and cardiac conduction disease in humans. J Clin Invest 2008;118:2260–2268.
36. Delpon E, Cordeiro JM, Nunez L, et al. Functional effects of KCNE3 mutation and its role in the development of Brugada syndrome. Circ Arrhythmia Electrophysiol 2008;1:209–218.
37. Hu S, Barajas-Martinez H, Burashnikove E, et al. A mutation in the β3 subunit of the cardiac sodium channel associated with Brugada ECG phenotype. Circ Cardiovasc Genet 2009;2:270–278.